processes

MDPI

Review

A Review of Thin-Film Growth, Properties, Applications, and Future Prospects

Subramanian Sakthinathan [1,2,*], Ganesh Abinaya Meenakshi [1,2], Sivaramakrishnan Vinothini [1,2], Chung-Lun Yu [1,2,3], Ching-Lung Chen [4,5,6], Te-Wei Chiu [1,2,*] and Naratip Vittayakorn [7]

1 Department of Materials and Mineral Resources Engineering, National Taipei University of Technology, No. 1, Section 3, Chung-Hsiao East Road, Taipei 10608, Taiwan; abimeenakshi1998@gmail.com (G.A.M.); vinodhinisakthinath@gmail.com (S.V.); samweo909li@gmail.com (C.-L.Y.)
2 Institute of Materials Science and Engineering, National Taipei University of Technology, No. 1, Section 3, Chung-Hsiao East Road, Taipei 10608, Taiwan
3 High-Value Biomaterials Research and Commercialization Center, National Taipei University of Technology, No. 1, Section 3, Zhongxiao E. Rd., Taipei 10608, Taiwan
4 Department of Safety, Health and Environmental Engineering, Ming Chi University of Technology, New Taipei City 24301, Taiwan; tommy@mail.mcut.edu.tw
5 Center for Environmental Sustainability and Human Health, Ming Chi University of Technology, New Taipei City 24301, Taiwan
6 Center for Sustainability and Energy Technologies, Chang Gung University, Taoyuan 33302, Taiwan
7 Advanced Materials Research Unit, Faculty of Science, King Mongkut's Institute of Technology Ladkrabang, 1 Chalong Krung 1 Alley, Lat Krabang, Bangkok 10520, Thailand; naratip.vi@kmitl.ac.th
* Correspondence: sakthinathan1988@gmail.com (S.S.); tewei@ntut.edu.tw (T.-W.C.); Tel.: +886-2-27712171 (ext. 2742) (T.W.C)

Abstract: This review article's primary aim is to discuss different thin-film deposition technique methods and their important uses. The histories of thin-film technology, thin-film growth, thin-film classification, and thin-film preparation techniques are also covered in this review article. The preparation and characterization of functional thin films and nanostructured materials, as well as various devices based on these materials and recent developments are also focused on in this review. The properties of the materials and several thin-film deposition techniques are also covered in this article. This review article also discusses the classification and application of thin-film sensors. Furthermore, the formation of thin films and their physical properties are impacted by deposition conditions such as pH, temperature, deposition time, and deposition parameters, which are analyzed. This article discusses how a wide range of potential uses in structural, mechanical, and protective coatings; sensing; energy storage systems; catalysis; optoelectronics; and biomedicine are made possible by the special qualities of thin films and nanostructured materials, including their high surface area to volume ratio, structure, surface charge, anisotropic nature, and tunable functionalities.

Keywords: thin-film technology; classification; deposition technique; thin-film sensors; parameters

check for updates

Academic Editor: Fabio Carniato

Received: 18 December 2024
Revised: 25 January 2025
Accepted: 11 February 2025
Published: 19 February 2025

Citation: Sakthinathan, S.; Meenakshi, G.A.; Vinothini, S.; Yu, C.-L.; Chen, C.-L.; Chiu, T.-W.; Vittayakorn, N. A Review of Thin-Film Growth, Properties, Applications, and Future Prospects. *Processes* **2025**, *13*, 587. https://doi.org/10.3390/pr13020587

Copyright: © 2025 by the authors. Licensee MDPI, Basel, Switzerland. This article is an open access article distributed under the terms and conditions of the Creative Commons Attribution (CC BY) license (https://creativecommons.org/licenses/by/4.0/).

1. Introduction

"Thin films" are film layers with thicknesses ranging from nanometers to a few micrometers that are deposited on substrates. A thin film can range in thickness from a nanometer to many micrometers [1]. Thin films are used to modify material surfaces or functional devices. The structure of a thin film, as evaluated at the nanoscale or micrometer scale, has a major impact on mechanical, optical, electrical, and thermal properties [2,3].

The primary characteristic of thin-film materials is their growing use in technology. Thin films are better understood in materials science and a wide range of applied and theoretical studies (Figure 1). In terms of materials science, thin films not only possess the properties of matter but also forecast the relationship between preparation techniques and material design [4]. Thin-film materials have been studied for energy and electronics applications such as electronic semiconductor devices, light-emitting diodes, thin-film solar cells, optical coatings, and thin-film batteries. In particular, the elemental composition of such films is of great importance because the structure and mechanisms are based on the materials. The preparation method used to make a thin film and the inherent growth factors of the film greatly affect the structure. The distinctions between thin films and thicker materials are determined by the thickness. Small changes in thin-film growth may result in additional changes in thin-film properties across the nano-to-microscale range [5].

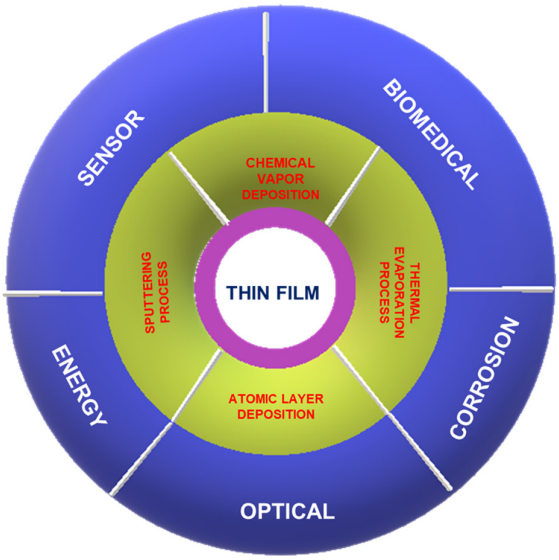

Figure 1. Thin-film preparations and their different fields of application.

Thin films are classified into two types: organic and inorganic thin films. The growth process and thin-film structure can be effectively modified to prepare thin films with specific properties. Thin films require vacuum technology to grow, and several vacuum coating methods have been developed for better growth dynamics. Such films are gaining popularity due to their high flexibility of application; the relatively low production costs of low-temperature processes, and their low-cost materials, which can be changed during processing [6].

Major analytical approaches have been employed to describe thin films, with a focus on their importance in facilitating the growth process. The various properties of thin-film materials must be identified to associate the qualities of thin films with specific growth conditions. These approaches are used to determine the material's size and nature, which requires a thorough understanding of the thin-film data. The correlation between parameters and thin-film qualities is critical. It should be noted here that the properties of a thin film are typically understood as the material's response to certain external stimuli [7,8].

The properties of thin films are the mechanical, thermal, magnetic, and deteriorative characteristics, as well as the dielectric constant, conductivity, and photoconductivity. The consequences of thin-film surface processes will have dominant effects on the results and result in the same optoelectrical responses. A variety of procedures can be employed to achieve material attributes. Some of these characterization techniques have led to more precise analysis of thin films and better knowledge of this class of materials [9].

Thin films have novel architectures, topology properties, high structural stability combined with a high surface area, excellent loading capabilities, improved optical/conductive properties, ordered and accessible porosity, versatile functionalization at pore sites, and an intrinsic pore surface. Thin films employed in sensing applications must meet particular requirements, such as simplicity of manufacturing with post-synthetic surface modification, a high aspect ratio, desirable conductivity, a large surface area, tunable porosity, and specificity to the target analyte. Thin-film materials have been developed in a variety of study areas, including energy, environmental, biomedical, and sensing applications [10].

Despite developments in multifunctional sensing devices, large-scale manufacturing is constrained by certain factors. To overcome these constraints, it is desirable to be able to manage a variety of material qualities, such as homogeneity, shape dispersibility, surface area, chemical stability, pore architecture, accessibility, and affinity. Thin films are commonly employed to enhance the surface characteristics of materials. A thin-film coating can improve transmission, reflection, absorption, resistance, corrosion, penetration, and electrical behavior. Thin films are inexpensive bulk materials that meet the criteria of materials required. Thin-film technology is used in micro-, nano-, and optoelectronics to reflect or fit the transmission of glass bodies. Thin-film technologies are classified into chemical vapor deposition (CVD) and physical vapor deposition (PVD) procedures [11].

Bibliometric analysis on the Scopus database revealed that 22,906 publications on thin-film sensors have been published since 1960. Additionally, the data show that China and the United States have prominent positions in the thin-film scientific literature. It is also noted that, with 7589 publications, the USA has been the most productive nation in terms of thin films, followed by China with 4511 publications. A comprehensive overview of thin-film publications by nation is presented in Figure 2 [12].

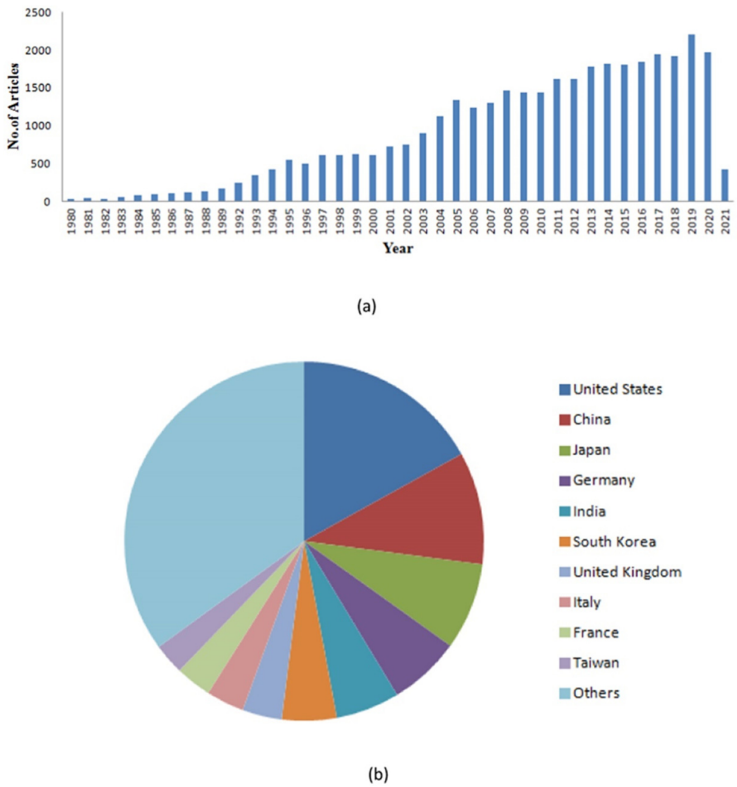

Figure 2. Global trends in thin-film technology: (**a**) representation of the year-wise publications of research articles indexed in the Scopus database; (**b**) geographical distribution of patents on thin films (reproduced with permission from reference [12] (open access).

2. Background of Thin-Film Technologies

The first thin-film coating was applied on a glass substrate to create a reflective surface when silver (Ag) was used as a thin-film material to create mirrors in Venice in the sixteenth century. Today, thin films are largely associated with semiconductors, which have a significant impact on numerous industries. Moreover, thin films are also renowned for their electrical properties, which result from material processing, and are employed in a wide range of electronic devices, optics, antireflection coatings, solar cells, interference filters, waveguides, flat panel displays, CDs and DVDs, and so on. Thin films have become key components of a wide range of energy storage devices, including solid oxide fuel cells (SOFCs), ultracapacitors, organic thin-film transistors (OTFTs), and sensors [12,13].

3. Thin-Film Growth

Several unique phases occur during the development of thin films, and each has an irreversible impact on the final film microstructure and physical properties. Nucleation by aggregation, random deposition caused by the aggregation of diffusing atoms, terrace diffusion, and atom potential upward are all important in thin-film growth [14]. Figure 3 displays a typical thin-film growth process that involves depositing atoms onto a substrate. All thin films undergo random nucleation, followed by growth stages. The earliest stages of thin-film growth include island growth, nucleation, coarsening, coalescence, and percolation. Thin-film growth based on deposition levels requires control of the thin-film growth temperature, pace, surface chemistry, nucleation, and growth phases [15]. In addition, external factors such as electron beams or ion bombardment can influence the nucleation process. Thin-film formation is influenced by the deposition process, microstructure, film tension, and associated defect structures. Moreover, thin-film deposition parameters determine the crystal phase and orientation of the resulting thin films. The reaction conditions, structure, and deposition procedure all affect the thermal and mechanical properties of thin films [16,17].

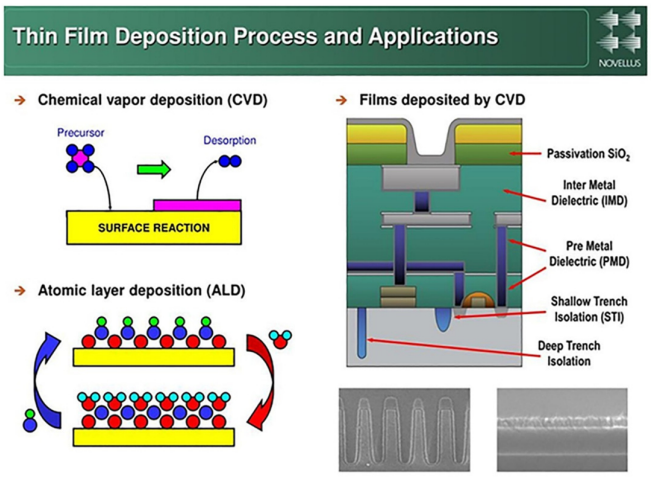

Figure 3. Thin-film deposition process (reproduced with permission from reference [18]).

4. Thin-Film Classification

Thin-film deposition does not occur in a liquid phase before hardening. For example, when warm wet air comes into contact with a cold windowpane, water vapor in the air immediately condenses into fine ice crystals, creating and applying a thin-film coating to the glass substrate. Metals, compounds, and metal oxides are all materials that can be used to create such coatings [19]. Magnetic, optical, thermal, chemical, mechanical, and electrical applications all involve thin films. Moreover, reflective and anti-reflective coat-

ings, solar cells, monitors, waveguides, optical detector arrays, insulators, semiconductor devices, integrated circuits, and piezoelectric motors are all produced from electrically thin sheets [20,21].

Figure 3 illustrates the three types of thin-film deposition based on the nature of the deposition. The thin-film approach relies on a physical or chemical process. The chemical process incorporates both solution deposition techniques and the gas phase. Gas-phase techniques include chemical vapor deposition, atomic layer epitaxy, and atomic layer deposition. Solution deposition techniques include the sol–gel technique, spin coating, spray pyrolysis, and dip-coating methods. Besides the above, magnetron sputtering, physical vapor deposition, pulsed laser deposition, and molecular beam epitaxy techniques are also used for thin-film synthesis [22,23].

The deposition methods include chemical bath deposition, anodic oxidation, electron beam deposition, advanced reactive gas deposition, and vacuum evaporation. Chemical vapor deposition (CVD) is a commonly used vacuum-based deposition process that produces high-quality and high-performance materials. In this technique, gas-phase precursors are used in a chemical process to form thin-film layers on a substrate. This process exposes one or more volatile precursors to the substrate surface to form a thin-film coating [24].

CVD is a process for producing non-volatile solid thin films on substrates requiring chemical interactions involving halide compounds, organometallics, and other gases. CVD differs from PVD in that it employs a multidirectional deposition process to deposit materials onto the substrate. CVD is widely employed in microfabrication methods to deposit materials in a variety of morphologies, including amorphous, monocrystalline, polycrystalline, and epitaxial ones [25,26]. The materials interact with the bulk surface, causing the chemical breakdown of some gas components and forming a solid coating on the base materials. CVD is employed in a variety of applications, including the deposition of materials on turbine blades to improve thermal, wear, and shock resistance. CVD techniques include plasma-enhanced, atomic layer, liquid-phase, epitaxy, microwave plasma-assisted hot filament, spray pyrolysis, and metal–organic filament deposition [27].

5. Thin-Film Preparation Methods

Various technologies are used for thin-film growth, including a wide range of alternatives when it comes to thin-film growth processes. However, these methodologies can be broadly classified into two types: bottom-up and top-down approaches [28,29].

Top-down approaches involve nanostructures with larger beginning structures that can be controlled from the outside. Lithography is a hybrid process in the semiconductor industry. In this process, thin films are grown from the bottom up and etched from the top down. Within these two techniques, there are three general categories for the synthesis of thin films and nanostructured materials [30].

Gas-phase processes, such as vapor deposition, flame pyrolysis, high-temperature evaporation, and plasma synthesis, are examples of the first group. Liquid-phase techniques and chemical reaction processes are employed in the second category to produce colloids. Among the last group of solid-phase processing techniques are hydrothermal, sol–gel, and electrodeposition processes, along with grinding, milling, and alloying. Ion implantation, ion beam mixing, cathodic sputtering, high-vacuum evaporation, ion plating, and pulse implantation plasma spraying techniques are also used for thin-film synthesis, as illustrated in Figure 3 [31,32].

6. High-Vacuum Evaporation Used in Five Different Evaporation Sources

Resistance-heated sources include anodic arc evaporators, cathodic arc evaporators, induction evaporators, and water-cooled Cu crucibles with various deflection angles.

Different conductive media are employed in thin-film development. Due to their great electrical conductivity, metallic nanoparticle (NP) paints are most commonly utilized to create conductive tracks [33,34].

Additionally, the inks are divided into three categories: metallic oxide NPs, core–shell bimetallic NPs, and single-element metallic NPs. One of the most significant inks among them is silver nano-ink, which has certain disadvantages, such as its extremely high cost, toxicity to humans, costly centrifugal separation, and the need for extensive solvent use because of the low metal precursor concentrations used [35].

Furthermore, producing tiny AgNPs with a high solution concentration is difficult. High concentrations of silver nanoparticles are synthesized by using non-hazardous chemicals and minimal power. Additionally, substrates having tensile loads are appropriate for the fabrication of strain sensors. In 2010, Jeong et al. reported the preparation of silver nanoparticles by chemical reduction and their utilization as a capping agent. The silver ink was discovered to have good dispersion stability [36].

Pudas et al. developed a rotogravure printing method for producing conductive lines on surfaces like paper and polymers. Moreover, silver nanowires are used because of their percolating network structure to create flexible and foldable conductors. Chen et al. combined the network connections that produce silver nanoparticles on nanowire junctions using a simpler reaction to increase the material's mechanical strength under extreme straining circumstances [37].

Other conductive materials are La-doped $BaSnO_3$ films, Nb-doped $SrTiO_3$ films, VO_2, and B-doped diamond thin films. To assess the frequency range in the semiconductor–metal phase transition, Jepsen et al. examined the dielectric characteristics of a thin VO_2 layer. Chen et al. created diamond thin films doped with B and examined their morphological and microstructural stability. Zhu et al. used laser molecular beam epitaxy to develop Nb-doped $SrTiO_3$ thin films on $SrTiO_3$ substrates and examined their microstructural properties. Terahertz characterization of La-doped $BaSnO_3$ (BSO) thin films was performed by Arezoomandan et al. to construct electromagnetic structures [38,39].

7. Thin-Film Deposition Methods

Thin-film deposition involves covering a substrate with a thin layer of material ranging from a few nanometers to 100 μm. It can also be used to build up layers on top of previously applied coatings. Thin-film materials for semiconductors, photovoltaics, CDs, disc drives, and optical devices are made using thin-film production techniques. A volatile fluid precursor causes a chemical change on the deposition surface, resulting in the deposited coating. Physical vapor deposition involves releasing a substance from a source and depositing it on a substrate using mechanical, electromechanical, or thermodynamic processes [18].

7.1. Chemical Vapor Deposition

Chemical vapor deposition (CVD) is a process that produces high-quality, high-performance solid materials. To generate non-volatile solid thin films on substrates, a chemical reaction occurs with an organometallic or halide compound to be coated. It is a liquid-phase equivalent of the well-known chemical vapor deposition, which occurs in the gas phase. The dissolved precursors commonly react with one another in an aqueous solution at low temperatures (30–808 °C). Experimental designs aim for uniform deposition with no pinholes [40,41]. An experimental setup is used to investigate the growth of films resulting from bulk precipitation of the solution. In this technique, the substrate remains stationary while the solution is agitated by a magnetic stirrer. The chemical bath is heated to the appropriate temperature with water or paraffin that is regularly agitated. While

stirring is frequently started at the target temperature, it may also be conducted constantly from room temperature [42].

This process yields solid materials of great purity. Metal catalysts are widely used in the production of semiconductors. When one or more vaporized precursors come into contact with the substrate, they adsorb at high temperatures. The adsorbed layer can be transformed into the required product through thermal or chemical (gas/vapor) methods. A gas flow eliminates the byproducts, and nucleation is homogeneous in the gas phase but heterogeneous in the solid phase [43,44].

7.2. Thermal Evaporation Process

Thermal evaporation generates vapor pressure by heating and evaporating a solid material that will be used to cover a substrate in a high-vacuum chamber. Even at low vapor pressures, a vapor cloud can form inside the vacuum deposition chamber. Thermal evaporation is a common PVD method that involves the use of resistive heating at high temperatures in a high-vacuum chamber to cause solid material evaporation and create high vapor pressure [45]. Then, the stream of evaporated material coats the surface of the substrate present in the vacuum chamber. The thermal evaporation technique of thin-film deposition has many industrial applications, including the creation of metal bonding layers in solar cells, thin-film transistors, semiconductor wafers, and carbon-based OLEDs. A thin film can consist of a single component or of co-deposited layers of different materials [46].

7.3. Sputtering

Sputtering involves bombarding a target substance with high-energy particles to deposit the substance on a substrate such as a silicon wafer. The target material to be deposited receives a negative electric charge, causing the plasma in the chamber to glow. The vacuum chamber is filled with the inert gas argon, followed by the substrates that will be coated. Atoms are "sputtered off" the target by reacting with the argon gas atoms, which carry the particles into the vacuum chamber and deposit them as a thin layer [47–50].

8. Thin-Film Synthesis Methods

There are various ways to group the synthetic methods that are used to prepare thin layers. Based on layer thickness, distinctions can be made in the classifications. The thickness range of ultrathin layers is $\geq$100 nm. These films are often deposited using a variety of methods, including electrochemical, chemical, and physical vapor deposition [51]. They have a more intricate architecture and a wide variety of synthetic pathways. Ensuring precise control over the size and shape of nanoparticles is crucial for the creation of intricate nanoscale layers possessing unique properties such as hydrogen storage, chemical reactivity, and biosensing [52,53]. The nanoparticles may come from semiconductors, insulators, metallic and magnetic oxides, and other material types. The difficulty arises with the upscaling of the preparation method, as in large-scale production, the cost, time, and quality of the layer could differ greatly from those factors on a small scale [54].

Vapor–solid deposition methods use heat, lasers, and plasma to create vapor as the reactant. This process includes radiofrequency sputtering, thermal evaporation, and laser-assisted catalytic growth. Chemical methods are also used for preparing thin films with nanostructures. Both established and novel methods are used to modify the chemical compositions of nanolayer molecules and atoms. The techniques consist of the combination of several chemical reactions that can occur in the solid, liquid, gaseous, and heterogeneous phases. In general, two approaches are used to produce thin films. A conventional approach for cutting, milling, and shaping particles employs external control; this could be solely physical or a combination of physical and chemical processes. It includes at least one

lithography and one etching phase. The chemical characteristics of individual molecules or microscopic particles can cause them to spontaneously arrange themselves into useful conformations [55].

8.1. Gas-Phase Fabrication

Generally, gas-phase manufacturing takes place under vacuum conditions. Based on the general synthesis circumstances, four approaches can be defined as follows in gas-phase fabrication [56].

1. Thermal vapor transport method: nanowires and nanorods are deposited in thin-film form via evaporation from supersaturated fluids.
2. Catalyst-assisted approach: A catalyst layer is applied to the substrate surface; this is a variation in the thermal vapor transport method. The catalyst must be chosen specifically, and the growing temperature is high.
3. Physical vapor deposition: PVD is a standard technique for thin-film deposition. It has multiple phases and produces ultrathin films.
4. Chemical vapor deposition: CVD is a popular approach for depositing thin films and nanostructures of a wide range of materials. It is useful for creating a variety of nanostructures, including carbon nanotubes, inorganic nanorods, and nanowires [57,58].

8.2. Liquid-Phase Fabrication

In liquid-phase fabrication, the synthesis takes place in an atmosphere with a relatively low temperature. The sol–gel process is a flexible solution process for producing glass and ceramics. As the name implies, the materials transition from a liquid solution to a solid gel. First, precursor solutions are synthesized based on the thin-layer composition and chemical procedure. Then, a homogeneous precursor layer of controlled thickness is created to coat the substrate. Finally, thermal treatment converts the deposited precursor layer into a crystallized final oxide layer, which may be either amorphous or nanocrystalline [59].

8.3. Electrochemical Deposition Method

The electrochemical deposition technique is commonly used for the deposition of metal and semiconductor thin films with nanometer-sized channels. The substrate is immersed in an aqueous metallic salt electrolyte. When a sufficient electric current is passed through the electrolyte, metal ions are reduced and deposited on the solid surface. Electrochemical atomic layer deposition is a unique technology [60].

8.4. Electrospinning Method

This method is commonly utilized for the production of micro- and nanofiber thin films. It can be used alongside the sol–gel approach. The setup consists of three parts: a high-voltage power supply, a small-diameter capillary tube, and a metal collector plate. This simple approach for creating ultra-structured thin films is illustrated in Figure 4. It includes both direct replication and partial replication approaches [61,62].

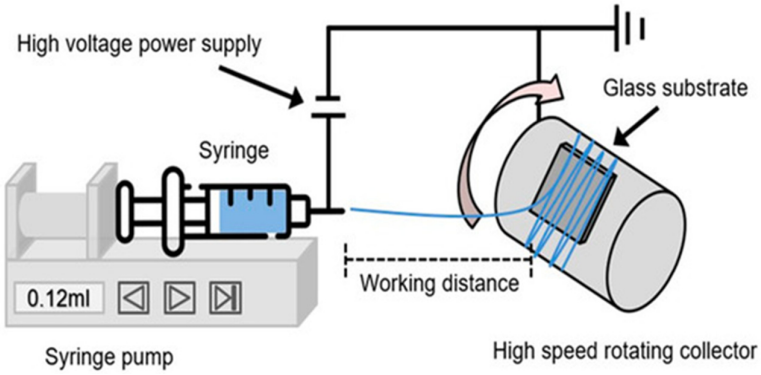

Figure 4. Schematic diagram of electrospinning experimental setup (reproduced with permission from reference [63]).

8.5. Glancing Angle Deposition

This is a modification of the physical vapor deposition system that includes both obligate and glancing angle deposition techniques. It can be used for the formation of vertically aligned nanorod arrays and helical nanostructures, the integration of multilayered nanorod structures with various morphologies/materials, and phase modulations (Figure 5) [63–65].

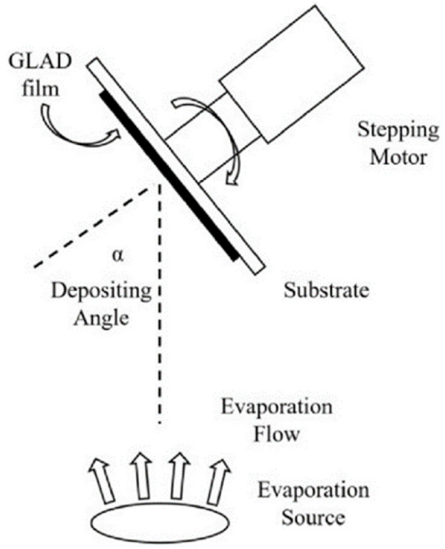

Figure 5. Diagram of glancing angle deposition film preparation (reproduced with permission from reference [64], © 2022 Optica Publishing Group under the terms of the Optica Open Access Publishing Agreement).

8.6. Chemical Precipitation

This is a simple bottom-up preparation method for nanostructured thin films containing nano-, micro-, and macroparticles. In a chemical process, insoluble particles are generated and precipitate onto the solid. This approach enables the creation of nanoparticles from various materials. The advantages of this preparation method are that it is inexpensive, does not require special equipment, and is recyclable. The chemicals can aid in the regulation of particle formation and development via variations in the pH, temperature, and concentrations of other organic molecules [66].

8.7. Hydrothermal and Solvothermal Synthesis

This process yields nanosized powders and thin films. A suspension or solution is maintained at elevated temperatures and pressures. Both effects influence the free energy of the phases while altering the solubility and reactivity of the reactants. The

outcome is unique structures on a solid surface. This synthesis is a dissolution–precipitation process [67].

8.8. Immobilization

Nanostructured materials have recently attracted much attention due to the possibility of creating new designs that can be used in a variety of sensing technologies. In addition to the usability of nanomaterials as identification elements in sensors, there is the possibility of the application of manipulation techniques in their development. Enzyme immobilization can be accomplished using four methods: physical adsorption, chemical adsorption, self-assembling monolayers, and the Langmuir–Blodgett film method [68].

8.8.1. Physical Adsorption

Physical adsorption is a simple and quick way to create enzymatic biosensors. It entails reducing the nanoparticles using a negatively charged ligand. The reduced gold nanoparticles then connect with the ligand, which protects the GNPs from electrostatic repulsion and provides stability. The resultant layer adds a negative charge to the colloidal particle surface. Although this procedure is faster and simpler than others, it may result in suboptimal alignments and lower functionality [69].

8.8.2. Chemical Adsorption

Chemical adsorption is the direct covalent interaction of the substance to be applied with the sensor surface. Chemisorption occurs through covalent contact between active groups and the gold surface [70].

8.8.3. Self-Assembly

During the self-assembly process, a layer with a well-ordered structure forms on a solid surface with no external orientation. Similar intricate processes can be seen in nature. The building blocks of these ordered layers, which could be atoms, molecules, and nano- and mesoscopic structures, are locked together via weak interactions such as van der Waals forces, hydrogen bonds, π-π interaction, covalent, metallic, and ionic bonding [71].

8.8.4. Langmuir–Blodgett (LB) Film

The Langmuir–Blodgett (LB) approach works by transferring insoluble monolayers from liquid–air interfaces to solid supports that intercept the liquid surface vertically. The LB approach is one of the most promising methods for creating nanolayer films, as it enables the precise regulation of monolayer thickness, homogeneous monolayer deposition over broad areas, and the ability to create multilayer structures with varied layer compositions. Another advantage of the LB approach is that monolayers can be formed on practically any type of solid substrate. The phrase "Langmuir film" typically refers to a floating monolayer at the air–water interface. Aside from being employed in monolayer investigations, the Langmuir film can also be used to create highly ordered multilayers of the amphiphile in question. Another characteristic of an LB layer is that its structure of the nanolayers generated from distinct amphiphiles on three different minerals (iron, copper, and mica) is highly similar, which indicates that molecules may stick to these solids [72–74].

9. Techniques for Layer Deposition

9.1. Spin-Coating Deposition

Spin-coating is a laboratory-scale process that involves depositing a small amount of solution into the center of a solid substrate and spinning the substrate at high speeds (1500–6000 rpm). This results in a homogeneous layer. The spin-coating technique is influenced by fluid viscosity and density. One advantage of the approach is that it produces

a homogeneous, high-quality coating. The downside is that it requires precise management and a clean atmosphere. Heating and UV/IR irradiation can be used to accelerate the process of the preparation of multiple layers. For example, the CuO/AlN film and $CuAlO_2$/AlN thin-film preparation procedures are presented in Figure 6 [75–77].

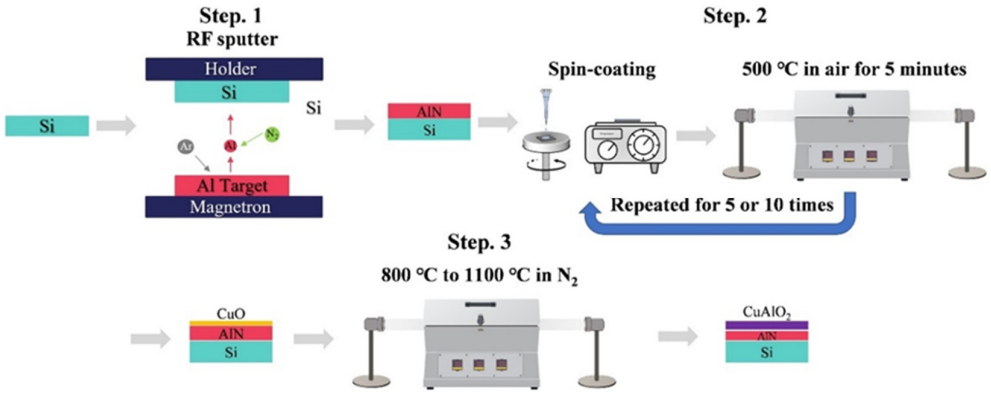

Figure 6. Illustration of the CuO/AlN film and $CuAlO_2$/AlN thin-film preparation procedures (reproduced with permission from reference [75]).

9.2. Spray-Coating Deposition

Spray coating involves transforming the coating solution into an aerosol using a pressure-driven atomizer with a nozzle. The solvent viscosity should be lowered. The droplets propelled by the carrier gas settle on the solid surface due to gravitation or an electrostatic field. Inkjet printing is a low-cost, industrial-scale technology that has promise for electronic sensing. In this scenario, a print head deposits small droplets onto a solid surface. Layer-by-layer technology creates nanostructured, multilayered nanocomposites with controlled structures at the molecular level. This approach is based on the alternate adsorption of molecular layers with opposite charges when a solid surface is dipped in solutions of cationic and anionic electrolytes in turn. The procedure is straightforward, and nanolayers can be used as biosensors by fixing biological molecules on their surfaces by electrostatic interactions. Polyaniline films are widely used as chemical sensors and biosensors due to their chemical stability, ease of manufacturing, and low cost. A liquid solution/dispersion of polyaniline generated by interfacial polymerization can be utilized to make a pH sensor modified with the layer-by-layer approach (Figure 7) [78–80].

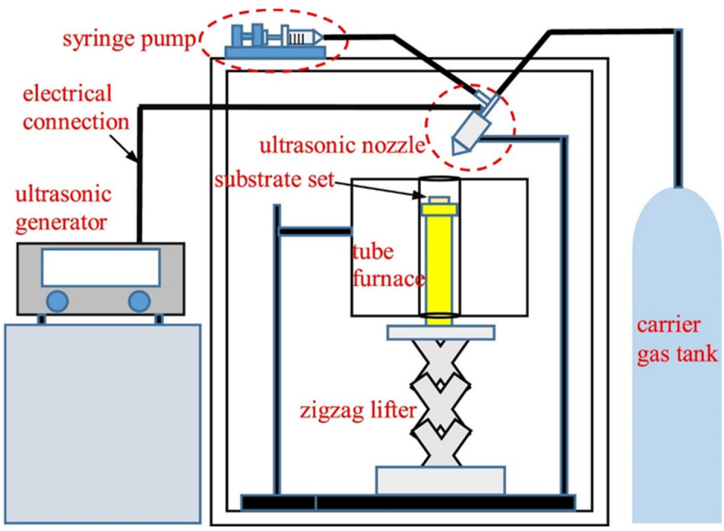

Figure 7. The ultrasonic spray pyrolysis system for LSBC thin-layer deposition (reproduced with permission from reference [78]).

9.3. Thin-Film Combinatorial Synthesis

Combinatorial synthesis techniques are increasingly being used to optimize a wide range of multicomponent functional materials. In the creation of thin-film materials, one of the most commonly utilized combinatorial synthesis methods established in the aforementioned collaborative initiative is combinatorial pulsed laser deposition. The pulsed laser deposition (PLD) method involves irradiation of a target material using an excimer laser (typically a KrF or ArF laser with λ = 248 or 193 nm) or a Q-switched Nd: YAG laser (third or fourth harmonic at 355 or 266 nm) (Figure 8). This irradiation of the target with high-intensity, short-wavelength lasers causes deposition on a substrate material. Combinatorial thin-film synthesis employs devices for exchanging several targets and rotating the substrate to create a process for fabricating the complete film, which is controlled by the system. Using this method, thin films with multiple compositions on the same substrate can be produced in a single pass [81].

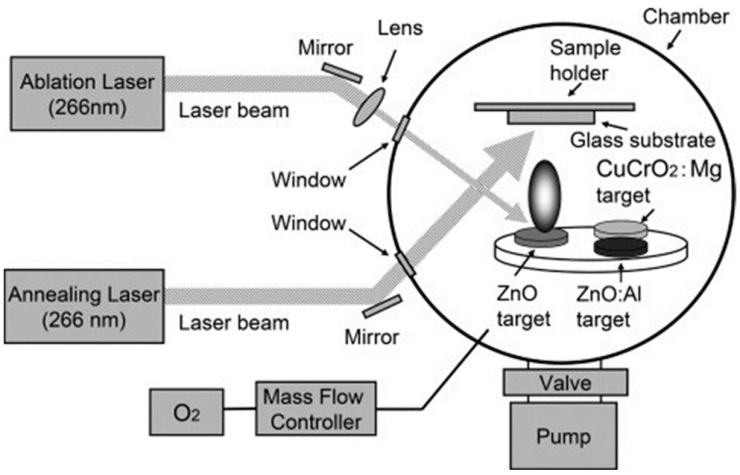

Figure 8. Schematic illustration of a PLD system employing in situ laser annealing (reproduced with permission from reference [81]).

Binary combinatorial thin-film production is conducted in two phases. In each step, a mask with a square-shaped hole moves at a consistent speed from one side of the substrate to the other, and then the target is changed. The moving mask allows for exact control of the film composition and thickness, resulting in a uniform fluctuation in composition.

The mask speed is calibrated in advance to optimize the amount of target material used and achieve a consistent film thickness, and the mask travels faster or slower based on the material's growth rate. The greatest film thickness achievable in a single cycle is normally one or one-half unit cells of the film material (0.3–0.6 nm), and switching between processes causes fluctuations in the film composition.

In a ternary system, the substrate can be rotated using a technique devised by the NIMS group. Following the deposition of each substance, the substrate is rotated by 120°. This method has the advantage of accurately determining the composition of each component. The PLD thin-film growth process is effective for producing oxides and nitrides [82–86]. However, this process is not suited for metal thin films due to issues such as the deposition of evaporated metal on the substrate in the form of droplets, caused by the thermal effect of laser irradiation. To address this challenge, the NIMS group devised a combinatorial metal sheet manufacturing process based on focused Ar ion beam sputtering.

This process employs separate ion-generating and film-forming chambers to maintain a high vacuum in the latter and prevent metal film oxidation. In this technique, the ion gun creates an ion current of 20–50 μA, which is a variation in the low-power ion gun used in traditional combinatorial PLD systems. The irradiation area is tiny, only 1 mm to 2 mm.

The gun can be used to create specimens with ternary composition gradients. Depending on the materials, level of research, and development, many synthesis processes can be used.

Molecular beam epitaxy (MBE), PLD, and ion beam sputtering can all be utilized to produce thin films in fundamental research when compositional accuracy is required. On the other hand, sputtering is suitable for narrow compositional ranges such as those found in the early stages of practical device production. Some modern combinatorial synthesis methods use masks in conjunction with vapor deposition, and these approaches are useful for studying a wide range of thin-film materials, including oxides, nitrides, metals, and organic compounds.

These approaches can be used to create high-quality, high-precision samples by selecting the best procedure for a certain film material and application. For example, multitarget sputtering is a physical vapor deposition technology that is widely employed in the fabrication of industrial production equipment due to its compatibility with a wide range of materials. However, when the plasma spreads throughout the deposition process, the material being deposited moves across the mask, making compositional fluctuations less accurate.

This is known as the wraparound effect. MBE, PLD, and ion beam sputtering produce highly straight flows of the material being deposited, resulting in minimized wraparound effects. The linearity of compositional changes in a film deposited by a focused Ar ion beam sputtering to a specimen is generated using the standard DC magnetron sputtering approach. This enhanced performance allows for the precise fabrication of ternary samples [87–92].

9.4. Chemical Solution Deposition

The chemical solution deposition (CSD) process involves producing thin films by using chemical reactions to deposit precursors. The usual processes in the process include solution preparation, film deposition, and gel-to-ceramic conversion. To complete the film deposition process, numerous coating methods, such as spin coating, dip coating, and spray coating, can be used. The morphology of the film is determined by the chemistry of the solution, so a solid grasp of chemistry is necessary to develop a practical solution. CSD is a nonvacuum, inexpensive method for producing thin films of polycrystalline, textured, and epitaxial oxide. Its many uses include superconductors, buffer layers, ferroelectrics, and magnetic and optical films. Additionally, CSD can be used in conjunction with other processing methods, including soft lithography and inkjet printing (Figures 9 and 10 and Table 1).

Table 1. Comparison of different preparation methods of thin film [52].

Preparation Method	Advantages	Limitations
Chemical vapor deposition	High throwing power, high deposition rate, flexible for designing	High-temperature supply, the organic exhaust gas is hazardous
Sputtering	Able to deposit a wide variety of materials for in situ cleaning, better film quality, and step coverage	Substrate damage due to ion bombardment or UV generated by plasma, more contaminations

Table 1. *Cont.*

Preparation Method	Advantages	Limitations
Physical vapor deposition	Harder and more corrosion resistant, ability to utilize any type of inorganic materials, environmentally friendly	Operates at high temperatures and vacuums and requires a cooling water system to dissipate large heat loads
Electrodeposition	Self-purification capability, improved interfacial bonding	H_2 embrittlement
Inkjet printing	Accuracy	Printing speed, lack of printed film uniformity
Molecular Imprinting Polymerization	Inexpensive, homogenous, stable, and selective	Slow binding kinetics
Spin coating	Layer thickness can be easily adjusted	Complex process
Dip coating	Low-cost layer thickness can be easily adjusted	Slow process, ability to block the screen
Sol–gel technique	Produce high-quality materials with homogeneity and purity at low temperature	Long processing time
Pulsed vapor deposition	Compatible and straightforward with oxygen and other reactive gases	Particulates, composition, and deposition depend on deposition conditions
Screen printing	It can be used on any substrate and irregular surfaces	Expensive and time-consuming

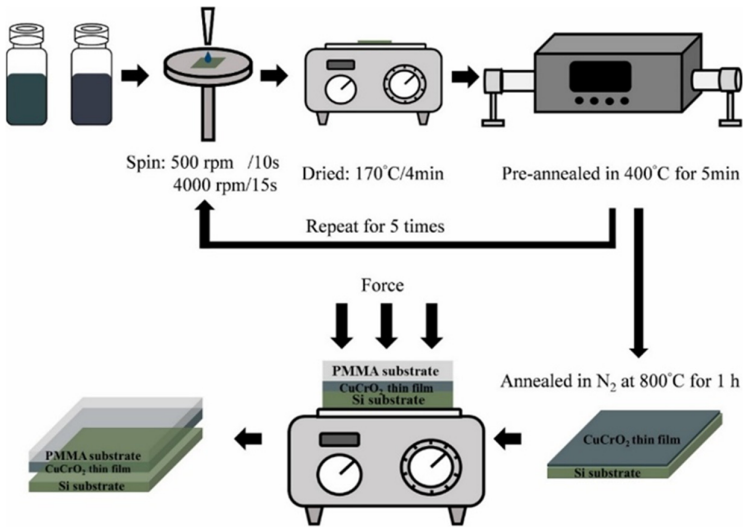

Figure 9. Schematic diagram of the preparation of the PMMA substrate/$CuCrO_2$ film/Si substrate (reproduced with permission from reference [91]).

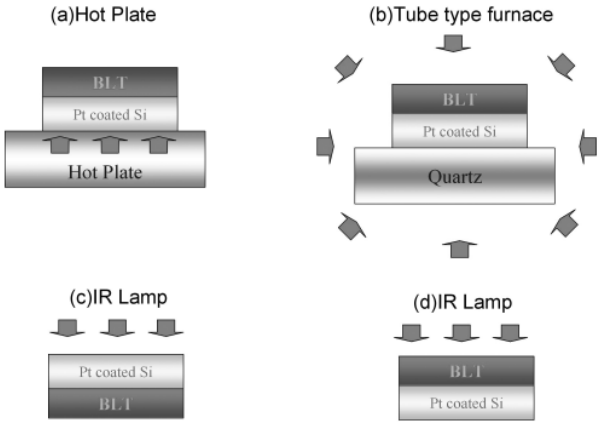

Figure 10. Scheme of various drying methods (reproduced with permission from reference [92]).

10. Thin-Film Sensors

These film-based materials are used for different sensor applications. Among the sensors that use thin films are gas sensors, pH sensors, chemical sensors, biomedical devices, temperature sensors, force sensors, pressure sensors, flow sensors, humidity sensors, and strain sensors. Below is a summary of some common examples of these sensors [26].

10.1. This Film Gas Sensors

Electronic devices called gas sensors are used to detect several gases, including ammonia, CO_2, SO_2, H_2S, CO, C_2H_5OH, and NO_2. They are frequently used to measure gas concentrations and detect harmful gases. Bruno et al. used chemical vapor deposition to create a tin oxide thin-film gas sensor. Weibenreider et al. used Hall measurements to examine the electrical characteristics of gas sensors. They discovered that when the oxidizing atmosphere decreases the electron concentrations, the resistance rises as a result. Another ZnO thin-film gas sensor was created by Mitra et al., who also looked into the electrical and gas-sensing capabilities of the device. It was discovered that oxygen adsorption on ZnO produced a surface with increased stability and resistance, both of which are necessary for the resistive mode of sensor operation. Using a micromachining approach, Tao et al. created a WO_3 thin-film gas sensor and studied its H_2S-detecting properties. Their findings demonstrated the greater sensitivity range and good response and recovery times of the platinum-doped WO_3 gas sensor. Chang et al. investigated the effects of the thickness and operating temperature of ZnO and Al thin-film gas sensors on CO gas sensing. The surface resistance of the thin film was used to investigate the qualities of gas sensing, and it was discovered that the structural features directly correlated with the sensing properties. Sheih et al. applied the sol–gel dip-coating process on an alumina substrate to create WO_3 and W-Ti-O thin-film gas sensors. Subsequent research on the effects of titanium doping revealed that the addition of titanium ions significantly increased sensitivity [93–96].

To detect ammonia gas, Prasad et al. produced a MoO_3 thin-film gas sensor and compared the ion beam deposition and sol–gel fabrication processes. Neodymium cobaltite ($NdCoO_3$) thin-film CO gas sensors were created by Malavasi et al. using rf magnetron sputtering, and the sensing characteristics were examined. Using the flash evaporation approach, Desai et al. created an indium sesqui telluride (In_2Te_3) gas sensor on a glass substrate. The properties of CO_2 gas sensing were also investigated. Stankova et al. used tungsten oxide thin films to build gas sensors. The process of radiofrequency (rf) sputtering was used to generate thin films. By evaporating a variety of dopant materials, including noble metals and metal oxides, the sensitivity to sulfur dioxide and hydrogen sulfide gases was examined.

A ZnO and Al thin-film sensor was created by Chou et al. to detect ethanol vapor. The outcomes showed increased reliability, sensitivity, and recovery time. A SnO_2-ZnO sensor for the detection of C_2H_5OH gas was created by Kim et al. and its sensing properties were examined. To detect ethylene gas, Jadsadapattarakul et al. created a SnO_2 thin-film sensor. By applying a layer of [010] plane highly preferred orientation silicalite-1 polycrystals, the authors were able to increase the sensing response, time of response, and recovery. A palladium-sensitized porous silicon (PS) hydrogen sensor created by Kanungo et al. demonstrated an improvement in the gas response at higher temperatures. To create quartz crystal microbalance (QCM) gas sensors, Lee et al. employed a method of TiO_2 and polyacrylic acid adsorption.

The purpose of that sensor was to identify amine smells. In 2010, Kim et al. developed SWNT-based sensors. Multiple spray coatings were used to deposit the thin film, and the response for alcohol vapor detection was examined. Similarly, numerous thin films based on CNTs have been employed to make gas sensors for formaldehyde and CO_2. By encasing a lipophilic, polynuclear gold(I) complex and bis{m (bis(diphenylphosphine) octadecylamine-P, P)} dichlorodi gold(I) in oxygen permeable polystyrene and ormosil matrices, Mills et al. (2011) created thin-film oxygen sensors, and their detecting properties were examined.

Polycrystalline ZnO–In_2O_3 thin films were created on glass substrates by Rambu et al., and their sensitivity to different gases was examined. A SnO_2 thin-film sensor, developed by Sharma et al., had a good response to NO_2 gas. Using the spin-coating technique, Chougule et al. created nanocrystalline ZnO thin-film NO_2 gas sensors. They investigated how the reaction was related to the operating temperature and concentration. Copper and platinum were sputtered together by Abburi et al. to develop nanoporous platinum thin films. In their work, the sensitivity was measured with different hydrogen concentrations using a resistance transient approach.

Additionally, the effects of temperature and pore size on response time and sensitivity have been investigated. Hazra et al. used UV-assisted anodization to generate a nanocrystalline TiO_2 thin film to create a hydrogen gas sensor. Tabassum et al. used thin sheets of ZnO and copper to create a H_2S gas sensor. It was noted that the sensor was highly sensitive and had an improved response time. Xie et al. developed reduced graphene oxide (RGO)/poly (3-hexylthiophene) bilayer films that were employed as active layers in gas sensors. Ganbavle et al. evaluated the influence of film thickness on a nitrogen dioxide gas sensor that was made using sprayed tungsten oxide thin film.

Using radiofrequency sputtering, Chou et al. created and demonstrated an ammonia gas sensor based on a p-type nickel oxide thin film. It was discovered to function better and have greater chemical stability than previous sensors of its type. Toan et al. used SnO_2 thin-film sensors to create H_2 sensing devices. They were also made more sensitive by employing tiny palladium islands. Sputtering and microelectronic techniques were used in tandem to create them. Therefore, based on the literature studies, thin-film materials are currently used for gas sensing in different fields of application [26,95–99].

10.2. pH Sensors

An instrument used to gauge the alkalinity and acidity of water and other liquids is a pH sensor. There is a high demand for tiny sensors that measure pH. As a result, numerous researchers have created thin-film pH sensors, some of which are presented here. An optical sensor was created by Allain et al. for high-acidity readings. The developed sensor was constructed by utilizing silica thin films doped with an acid indicator. pH-monitoring thin-film transistors were created by Caboni et al., and Chien et al. used carbon nanotube (CNT) thin film to build extended-gate field-effect transistors (EGFETs). The new sensor

showed enhanced electrical and sensing capabilities. Nanostructured EGFET pH sensors were created by Chiu et al. using a nano-rod array and zinc oxide thin films. Liu et al. used indium tin oxide to create pH sensors. A dual-gate thin-film transistor with enhanced pH sensitivity was created by Kumar et al.

Lu et al. created an InGa-ZnO ion-sensitive thin-film transistor sensor employing a high-sensing membrane that was manufactured via low-temperature atomic layer deposition. A high-sensitivity amorphous $InGaZnO_4$ thin-film transistor (a-InGaZnO TFT) based on the top-gate effect was created by Takechi et al. for use in pH sensing applications. In their study, Chou et al. employed nickel oxide (NiO) as the sensing film for a flexible arrayed NiO pH sensor. They found that adding oxygen gas during the sputtering deposition process increased the sensor's average sensitivity.

A bi-electrode thin-film sensor that was both pH- and redox-sensitive was created by Iken et al. to detect both parameters simultaneously in aqueous solutions. The structure and sensing properties of nickel oxide sensing films used as extended-gate field-effect transistor pH sensors were investigated by Pan et al. in 2021. It was discovered that, after post-deposition annealing at 500 °C, the pH sensitivity of the NiOx sensing film increased [26,100,101].

10.3. Bio-Medical Sensors

Thin-film sensors offer several benefits, such as improved mechanical flexibility and increased sensitivity. Thus, they are utilized in biomedical electronics and wearable technology, among other things. A sensor system was created by Bae et al. utilizing electrically conductive materials. It contained non-toxic oligosaccharide molecules and carboxylated polypyrrole, which were combined with biocompatible hydrogels. Jiang et al. used hydrogel and functional DNA to create a capillary sensor. A DNA hydrogel sensor was created by Wang et al. and utilized to visually quantify micro-RNA. Song et al. used conductive cellulose nanocrystals to create biocompatible hydrogel sensors. Liu et al. used DNA-inspired wet adhesion and anti-freezing approaches to create a hydrogel-based skin sensor. Liang et al. developed a hydrogel sensor demonstrating great efficiency in monitoring glucose. Liu et al. created a strong hydrogel and used molecular springs to increase its strength. Therefore, based on the aforementioned works, thin films are used for biomedical applications in different fields [26,102–105].

10.4. Chemical Sensors

Chemical sensors are widely utilized in industries such as the automotive, aerospace, food, and medical industries because they are capable of detecting a variety of substances. Semiconducting and conducting polymers are used in the majority of modern chemical sensors because of their benefits in terms of cost, mechanical performance, and compactness. Chemical sensors rely on the polymer's ability to change physically when exposed to chemicals. Yang et al. used alternating adsorption of charged species to create films of calixarene and polyelectrolyte. Thin films of molecular squares based on rhenium were employed in sensors by Kefee et al. to identify chemical substances. Using thin films of p-CuO/n-ZnO hetero-contacts, Dandeneau et al. created chemical sensors, optimizing characteristics like porosity and crystallinity. By thermally sublimating Zn-TIPP and first depositing silver, Sayyad et al. created a Ag/ZnTIPP/Ag sensor. The constructed sensor had good response and recovery, but it also displayed considerable hysteresis. Hussain et al. used quartz crystal microbalance (QCM) to analyze the sensor features while examining the binding behaviors of two distinct polymers. Yang et al. used thin-film organic field-effect transistors to construct a chemical vapor sensor. Xu et al. created graphene-based thin films for alcohol detection. A PANI–ZnO nanocomposite thin film was created by Paulraj et al.

to detect methanol at ambient temperature. A ZnO thin film sensor doped with Au was created by Deshwal et al. to detect acetone. After analysis of the response, it was found that there was good sensitivity along with faster reaction and recovery times. Based on the aforementioned works, different kinds of thin films are used as chemical sensors in various fields [106–109].

10.5. Temperature Sensors

A temperature sensor is a device used to measure the temperature by translating the input data into electronic data to monitor temperature changes. Thin-film temperature sensors include thermistors and resistance temperature detectors, among others. Thermocouple sensors embedded with polyimide were created by Mutyala et al. and subsequently migrated onto thin copper foils from glass substrates. Lithium battery temperature was monitored using these sensors. Using RF magnetron co-sputtering to deposit nickel and chromium thin films, Eom et al. created a temperature sensor that responded strongly to temperature. Thin-film temperature sensors were used by Ebner et al. to detect the temperature of hydrodynamically lubricated (EHL) contacts. ZrO_2 and Al_2O_3 substrates were used to construct platinum thin-film sensors. Using hydrogel films and bacterial cellulose for reinforcement, Hou et al. created a leaf-shaped sensor that they utilized to detect steam. A temperature sensor based on hydrogels and composite multi-wall carbon nanotubes (MWCNTs) was created by An et al. in 2020. It was discovered that the hydrogel's sensitivity to temperature was increased by the inclusion of carbon nanotubes. Another hydrogel-based temperature sensor that could retain water, withstand cold, and be remolded was created by Li et al. in 2020. A silver–carbon nanotube (CNT) nanocomposite film sensor was created by Sarma et al. in 2021. That sensor was shown to have a better temperature coefficient of resistance based on the findings. The above explanations provide the specifics of temperature sensors using thin films [109–113].

10.6. Force Sensors

Force sensors give robots input to help them feel and react appropriately, and they are widely used in many automated industrial applications. Nadvi et al. used micromachining to create force sensors with thin-film nickel-chromium piezoresistors. To quantify grinding operations, Dumstorff et al. created thin-film force sensors that were combined with steel. Luo et al. used worktables integrated with polyvinylidene fluoride (PVDF) to measure cutting forces during milling operations. In a similar vein, Liu et al. used thin-film sensors installed in fixtures to assess the cutting forces of milling operations. Hence, these film materials are used in force sensors in different fields of application [114–117].

10.7. Pressure Sensors

Gas tanks, oil pipelines, water supply systems, and turbine engine chambers are just a few of the systems that use pressure signals for process management. They are also utilized in commonplace applications such as health monitoring gadgets and smartphone touch screens. An electronic pressure sensor, which transforms the mechanical displacement into an electric signal, is typically used to detect pressure. There are five different types of transduction mechanisms: resistive, piezoresistive, electromagnetic, piezoelectric, and capacitive. Thin-film micro-diaphragm pressure sensors for high-temperature and -pressure situations were studied by Asadnia et al. To detect human motion, Jing et al. created hydrogel-based sensors based on cellulose nanofibril and polyvinyl alcohol. These sensors were found to be extremely sensitive to variations in pressure. Shin et al. created a wearable, wireless heart rate monitor using PVDF thin films and a ZnO nanoneedle. Lim et al. used n-type doped silicon to create a low-pressure sensor. Li et al. built a piezoresistive-based pressure sensor utilizing CNT–polyimide nanocomposites. The sensitivity and the

gauge factors were examined in their study. The outcomes showed the pressure sensor to have a high level of sensitivity and good flexibility. Kuoni et al. created a polyimide membrane with a ZnO piezoelectric thin-film pressure transducer and employed it as a liquid flow sensor that sensed differential pressure. Using conductive polymer film, Pan et al. created an ultra-sensitive pressure sensor with good repeatability, stability, and reaction time. To monitor pressure, Zang et al. created thin-film transistors. Using a piezoelectric polyvinylidene difluoride tetrafluoroethylene copolymer film, Sharma et al. also created pressure sensors [118–122].

10.8. Humidity Sensors

The humidity in an environment is measured using a humidity sensor. The results are transformed into an electrical signal. $BaTiO_3$ ceramic thin films were synthesized by Yuk et al. via sol–gel processing, and their humidity-sensitive characteristics were examined. A digital moisture measuring device utilizing porous silicon (PSi) was proposed by Islam et al. In 2015, Mittal et al. created a thin-film surface acoustic wave (SAW) humidity sensor based on porous metal oxide. A capacitive thin-film sensor was created by Mahboob et al. to detect moisture in gases. A printed electronics and silicon-based aerosol jet sensing platform was created by Clifford et al. In that work, an aerosol jet was used to deposit an interdigitated silver nanoparticle electrode as a layer that was sensitive to humidity. Su et al. used inkjet printing technology to create a PEG/gold nanoparticle thin-film humidity sensor. Sobhanimatin et al. demonstrated a new quick colorimetric humidity sensor employing the opal hydrogel composite (OHC). To create a three-dimensional opal photonic crystal, a highly monodisperse polystyrene (PS) latex was created by utilizing soap-free emulsion polymerization and coated on a glass substrate. The aforementioned studies confirm that thin-film materials are used for humidity sensing [123–126].

10.9. Strain Sensors

The main purpose of strain sensors is to track significant deformations and human activity. A thin film was used by Jiang et al. to create a straightforward strain sensor. The thin film in this sensor functioned as a fiber-optic interferometer. Thin-film strain gauge sensors were created by Stephen et al. to monitor ion propulsion. The microscopic magnetic characteristics of a stress sensor made using FeCoBSi thin films were assessed by Frommberger et al. in 2005. Two types of semiconductor strain sensors, namely micro-crystalline silicon and gated amorphous silicon, were created by Zhou et al. Polyimide substrates were used to create these sensors utilizing silicon thin-film transistors. In 2009, Kuo et al. and colleagues examined how strain affected the characteristics of polycrystalline silicon transistors grown on stainless steel foil. The sensitivity of a strain sensor made using FeSiB magneto-restrictive thin film was investigated by Suwa et al. Another strain sensor was created by Wang et al. using composites of polyimide and single-walled carbon nanotubes (SWCNTs). A strain sensor that could be powered by a light source was created by Yao et al. Luo et al. used thin-film polyvinylidene fluoride (PVDF) sensors to track the deflection in a milling process. A strain sensor was created by Yao et al. to measure significant deformations. In that work, polydimethylsiloxane (PDMS) composite thin films and CNTs were used to create the sensor. A temperature mechanical dual-parameter sensor with a PET/vanadium dioxide (VO_2)/PDMS multilayer construction was created by Liao et al. A strain sensor based on the surface acoustic wave (SAW) concept was created by Li et al. in 2019. The piezoelectric single-crystal PMN-PT thick sheet utilized in this strain sensor greatly increased sensitivity. To measure human mobility, Dai et al. created strain sensors employing hydrogel. To detect huge motions and physiological activities, Gao et al. developed a strain sensor employing sticky polyacrylamide hydrogel

that was driven by amino acids. Sun et al. created flexible strain sensors by using hydrogel reinforced with carbon nanotubes. In a similar vein, other scientists have created strain sensors for tracking human movements out of hydrogels and carbon nanotubes. Wang et al. introduced graphene to increase the sensitivity of an ion-conductive hydrogel. Based on the aforementioned studies, different thin-film materials are used in strain sensors [127–129].

11. Thin-Film Application

Thin-film sensors find extensive usage in a variety of fields, including biomedicine, physics, aeronautical engineering, and optics [130–132].

11.1. Biomedical Applications

Thin-film technology is employed in biomedical applications to create flexible digital X-ray detectors and flexible screens, which reduce manufacturing costs and improve the functioning of wearable biomedical devices. In biomedical applications, thin-film sensors are mostly used to detect radiation, heart rate, and blood sugar levels. An InSb thin-film sensor was created by Togawa et al. for use in biomedical applications. The impact of γ-rays on the optical characteristics of pure and mixed oxide materials was examined by Arshak et al. Alpuim et al. created thin-film piezoresistors made of nanocrystalline silicon. Their study involved the fabrication of sensors by hot-wire chemical vapor deposition on polyimide foils. A photo-plethysmograph biosensor was created by Smith et al. for optical tracking of heart rates. Using PVDF films, Vazquez et al. created a phonocardiogram. Zheng et al. created a poly (dimethylsiloxane) thin-film electrocardiography (ECG) sensor patch. A thin-film polyethylene terephthalate (PET) electrochemical sensor was created by Wang et al. to measure the amount of glucose in perspiration.

To create muscle skin sensors, Chen et al. created a hydrogel-reinforced cellulose skeleton by treating it with an alkali. In 2020, Sawayama et al. created a hydrogel glucose sensor capable of tracking glucose levels constantly. Injectable polymer hydrogels are also utilized in the bio-tissue synthesis of wearable Internet of Things sensors. Kim et al. created a tremor sensor for Parkinson's disease based on a hydrogel of catechol, chitosan, and diatoms. Based on these studies, thin-film materials are used for different kinds of biomedical applications [130–134].

11.2. Corrosion Applications

Corrosion sensors are used in conjunction with corrosion control techniques such as cathodic protection (CP) and corrosion inhibitors to monitor the corrosion behavior of structures. For decades, several corrosion sensors or probes have been used in corrosive settings. Some features that a corrosion sensor should have include ease of measurement, the ability to determine the rate of corrosion, a broad variety of applications, and a quick response time. The optical and electrochemical characteristics of Fe thin-film-coated optics for corrosion monitoring were studied by Wright et al. in 2021.

The galvanostatic deposition was used by Sanmugam et al. to create chitosan–zinc copper oxide composite thin films. They underwent additional testing to determine their corrosion, morphological, and structural characteristics. CNT–polyelectrolyte thin films were employed by Loh et al. to detect corrosion and strain. An iridium oxide film pH microsensor was created by Zhu et al. using a Pt ultra-microelectrode. In 2016, Rahmati et al. improved the corrosion and wear properties of the Ti-6Al-4V alloy by using a ceramic tantalum oxide thin-film layer. Li et al. used DC magnetron sputtering deposition to create a steel thin-film corrosion sensor. Therefore, thin-film materials are used in various ways for corrosion applications [135–138].

11.3. Optical Applications

Optical applications are a major area in the use of thin films. Yao et al. created a method for creating torsional micromirrors supported by single-crystal silicon. The created mirrors were composed of totally suspended single-crystal silicon grids with a layer of supporting oxide on top of a sputtered aluminum sheet. A Pb-based ferroelectric thin-film actuator was created by Sakata et al. for use in optical applications. For electro-optic applications, Shkir et al. studied the MZO/FTO thin-film system, created using the spin-coating approach, in terms of the system's linear, third-order nonlinear, and optical limiting. Based on their findings, MZO films appear to be superior candidates for optoelectronic uses [139].

For nonlinear optical applications, Constantinescu et al. and Ozcariz et al. suggested using optically transparent and electrically conductive indium gallium zinc oxide (IGZO) thin films to create optical fiber refractometers based on lossy mode resonance (LMR). To create a selective filter for optical applications, Khalil et al. synthesized and investigated the optical characteristics of alizarin yellow GG-Cu (II)-PVA nanocomposite film. A pH optical sensor based on thin sol–gel films containing bromocresol purple was created by Timbo et al. Abood et al. used a straightforward colloidal suspension to create a niobium pentoxide thin film for optoelectronic use.

Using pulsed laser deposition, in 2006, Caiteanu et al. produced thin coatings of titanium dioxide and tungsten trioxide for use in optical gas sensing applications. In 2014, Matei et al. suggested employing a Nd: YAG pulsed laser device to create high-quality, nanometric-sized ferrocene thin films on silicon- and ITO-coated glass substrates through matrix-assisted pulsed laser evaporation (MAPLE). In 2008, Manera et al. investigated the optical gas sensing characteristics of virgin TiO_2 thin films in combination with sol–gel-prepared gold nanoparticles (NPs) structured like dots and rods. These above studies show that thin-film materials are used as optical application materials due to their superior performance [140–142].

11.4. Energy Applications

Thin films have found extensive application in energy harvesting devices, including solar cells, photovoltaic cells, and thin-film batteries. Thin-film batteries are ideal for energy harvesting devices like solar cells and piezoelectric devices because of their excellent cycle life and flexible charging models. These devices transform mechanical vibrations into electrical energy. They are used in forestry terrain, structures, etc. Because they do not require an external voltage source and have high electromechanical coupling, piezoelectric vibration-to-electricity converters are widely used. Piezoelectric thin films are highly advantageous in a wide range of applications, including sensors, actuators, and high-energy-density harvesters. On silicon substrates, in 2009, Reilly et al. created a thin-film piezoelectric microscale energy scavenging device. Magnetoelectric (ME) heterostructures for electromagnetic energy harvesting on silicon cantilevers, comprising FeGa and $Pb(ZrTi)O_3$ piezoelectric thin films, were studied by Onuta et al. A piezoelectric energy harvester that utilized mechanical energy in shoes was created by Zhao et al. Iranmanesh et al. prepared a wearable piezoelectric energy harvester by fusing a dual-gate thin-film transistor with a PVDF piezoelectric charge generator. For use in energy applications, Hota et al. constructed integrated thin-film transistor rectifiers and micro-supercapacitors. Therefore, based on the aforementioned applications, different kinds of thin-film materials are used in the energy sector [143–146].

11.5. Antimicrobial Properties

Microbes are a major concern in the food, textile, water treatment, and healthcare sectors. Thus, one of the main challenges facing the research community is the development of an effective method to control harmful microorganisms. Using thin films and other antimicrobial systems aided by nanotechnology is a good substitute for killing bacteria or preventing them from sticking to surfaces. Because thin films can improve the beginning of drug actions, improve target drug distributions, decrease dose frequency, increase medication efficacy, and minimize microbial resistance and host adverse effects, they are thought to be particularly practical drug delivery strategies. Another great platform for incorporating nanostructured microbial drugs is membranes, a related class of flat sheet materials having molecular permeability capabilities. Thin-film structures with intrinsic or nano-assisted microbicidal properties are known as antimicrobial thin films (ATFs). Because of their many uses in a variety of industries, particularly in wound dressing, food packaging, textile finishing, and anti-fouling water treatment membranes, they are growing in popularity [147].

By modifying their functioning to target particular microbes in a variety of tailored designs, ATFs can be utilized to stop the growth of dangerous pathogens like bacteria and fungi on a range of surfaces. The nature of the active agent material, its stability against external environmental triggers, manufacturing processes, geometric requirements for adherence to a substrate material/surface, physical advantages such as breathability, application suitability, release patterns, toxicity limits, and exhaustive compatibility against interacting particles and with the host material are just a few of the many factors that must be carefully taken into account when designing the perfect antimicrobial thin film. Thin films are frequently utilized for antimicrobial activity, which is the mechanism of action behind nano-enabled antimicrobial thin films [148].

Thin films frequently cause membrane permeance, cytoplasmic leakage, and bacterial death by first adhering to anionic lipid head groups in the negatively charged membrane surface of bacteria through electrostatic interactions and then successfully inserting their hydrophobic groups into the non-polar bacterial membrane. Active compounds may also operate by dissolving into cells through electrochemical transduction mechanisms or by penetrating microbial cell membranes through oxidation reactions. There is great discussion of the many classes of nanostructured thin-film materials that have antibacterial qualities either through natural means or due to nanotechnology. Research on processing techniques and design strategies for integrating antimicrobial agents into useful thin-film-based delivery systems is described for each class of materials. Also covered are the methods of action against microorganisms and their use in various regions where microbial prevalence is prevalent. Chiu et al. reported the antibacterial property of $CuCrO_2$ thin films prepared by RF magnetron sputtering deposition, as shown in Figures 11 and 12 [47,147,148].

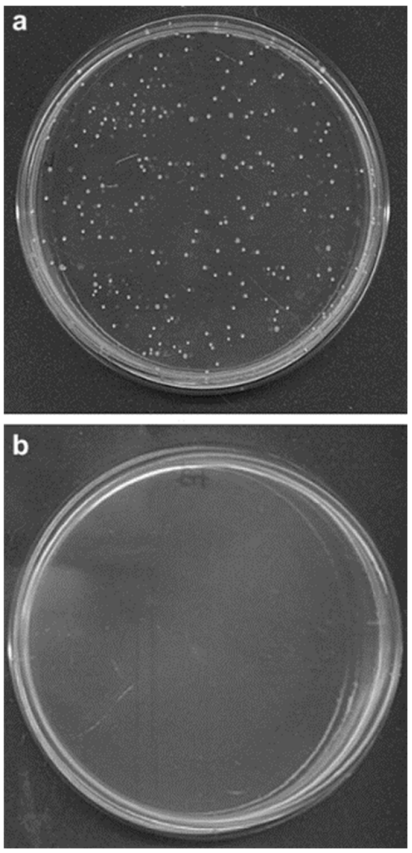

Figure 11. Test results on *E. coli* after 12 h: (**a**) incubated with blank glass substrate, (**b**) incubated with $CuCrO_2$ (60 nm)/glass (reproduced with permission from reference [47]).

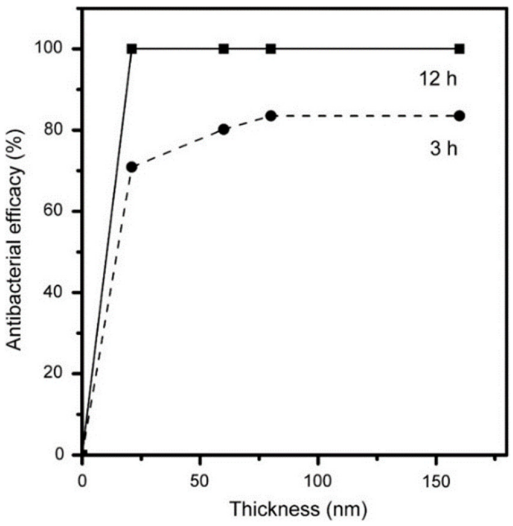

Figure 12. The antibacterial efficacy against *E. coli* incubated on $CuCrO_2$ film surfaces of various thicknesses (reproduced with permission from reference [47]).

12. Characteristics of Thin Films Affected by Deposition Conditions and Impact of Deposition Parameters

In solution deposition techniques, factors such as the substrate temperature, surface chemistry, solvent type, and solution concentration significantly impact the microstructures of thin films. The solution concentration is a key factor affecting thin-film coverage. At low concentrations, thin films often show poor coverage, resulting in a sub-monolayer with limited connectivity. Conversely, higher concentrations lead to the formation of mesh

layers and multilayers, which improve coverage and interconnectivity. This effect is evident in spin-coated and dip-coated copper phthalocyanine (CuPc) films. At lower solution concentrations, CuPc molecules typically create a sub-monolayer of interconnected ribbons, which are generally 20–50 nm wide, about 100 nm long, and approximately 1 nm thick. As the concentration of the solution increases, the film structures become more complex, showing better coverage and enhanced connectivity. Therefore, fine-tuning of the deposition parameters is essential to achieve the desired film characteristics and performance. As the concentration of CuPc in the deposited solution increases, the formation of multiple layers becomes apparent. However, due to the anisotropic properties of CuPc, achieving complete coverage with a single layer is challenging, as the anisotropy affects surface diffusion and the subsequent nucleation process [147–152].

The selection of a solvent is a critical choice in the solution deposition process for creating thin films. The evaporation rate of the solvent governs the crystallization rate, which subsequently affects the film's final morphology and microstructure, as illustrated in Figure 13. Solvents with high evaporation rates, such as chloroform, often lead to films with increased surface roughness because they form distinct clusters. The rapid evaporation leaves minimal time for the molecules to move or diffuse on the substrate, resulting in films with lower aggregation and less cohesive structures. On the other hand, solvents with slower evaporation rates, such as dimethylformamide, allow more time for molecular movement on the surface, leading to a more densely packed and orderly film. This has been demonstrated with tetrakis-(isopropoxy-carbonyl)-copper phthalocyanine (TIP-CuPc) and other small semiconducting molecules, illustrating how solvent choice can significantly influence the characteristics of the resulting thin film [153–156].

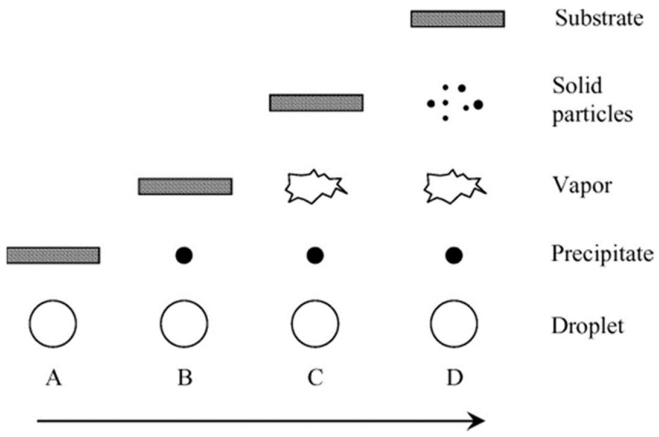

Figure 13. Description of the deposition processes initiated with increasing substrate temperature (reproduced from Thin-Film Deposition Using Spray Pyrolysis).

13. Growth of Thin-Film Metal Phthalocyanines: Thin-Film Formation, Microstructure, and Physical Properties

13.1. Nucleation

Vapor deposition is a widely used technique for creating thin films, primarily due to its reliance on heterogeneous nucleation (Figure 14). This process involves the condensation of adatoms on a substrate composed of different atoms than those present in the vapor phase. In this context, different stages are involved in the development of thin films. Nucleation takes place at elevated supersaturations, denoted by the formula

$$S = p/p_e \quad (1)$$

where po is the substrate material's equilibrium vapor pressure at temperature TS and p is the vapor pressure of the deposited material that evaporated from the source at temperature T. Deposition rate R and p are connected as

$$R = p/(2\pi mKT)1/2 \quad (2)$$

where the evaporation source temperature is T, the molecular weight of the deposited material is m, and K represents Boltzmann's constant. Nucleation occurs in a nonequilibrium state within a Wilson chamber, primarily due to the exceptionally high supersaturation levels, typically in the range of S = 105–1050. Mean-field nucleation theory offers a comprehensive explanation for this phenomenon.

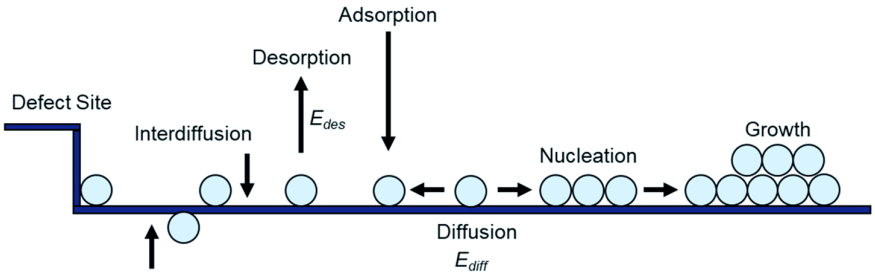

Figure 14. Schematic diagram of nucleation and growth process on a substrate. Reproduced from reference [11].

The process of forming nuclei and their subsequent growth is fundamental to the development of thin films, as in all phase transitions. Depending on the interaction energies between the substrate and the film atoms, one of three growth modes can occur, as illustrated in Figure 4 [157].

Layer by Layer: In the two-dimensional Frank–van der Merwe mode, layers of material grow one on top of another. In this mode, the interaction between the atoms of the film and the substrate is stronger than the interaction between adjacent film atoms.

Island Growth: In the Volmer–Weber mode, distinct three-dimensional islands form on the substrate. Here, the film atoms interact more with each other than with the substrate or adjacent film atoms.

Island + Layer: The Stranski–Krastanov approach involves the formation of individual islands after the deposition of one or two monolayers, combining aspects of both layer and island growth. Growth modes can be systematically categorized based on surface energies, with Young's equation as a key consideration.

In island growth ($\varphi > 0$), the formation of discrete islands occurs, while in layer growth ($\varphi = 0$), material builds up continuously (Figure 15). Layer-plus-island growth arises because the interface energy tends to increase as the film thickness increases; typically, the layer above the substrate is under strain to conform to the substrate's dimensions. The growth mode is influenced not only by interface energies but also by the level of supersaturation. Generally, as supersaturation increases, the growth mode shifts from island formation to layer growth [158,159].

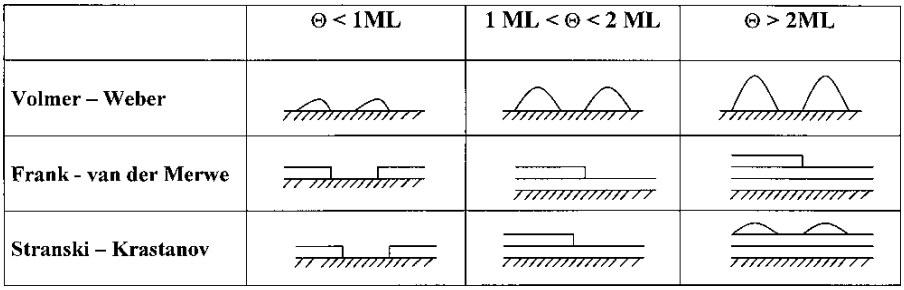

Figure 15. Initial states of film growth and substrate surface coverage in a monolayer (ML) (reproduced from reference [159]).

13.2. Coalescence

The next phase in the development of three-dimensional films involves the expansion of islands until they connect to create a continuous network. This coalescence process is crucial for designing films with specific properties. After two islands undergo solid-like coalescence, there may still be a grain boundary between them, or they might merge seamlessly to form a larger island without such a boundary. These processes are influenced by surface energies and supersaturation, and they involve material movement through surface and bulk diffusion. The transition from isolated islands to a continuous macroscopic network can be characterized by the percolation threshold thickness. Percolation refers to the process of something flowing through a permeable medium. This concept is particularly relevant when measuring electrical conductivity between two macroscopically separated contacts on an insulating substrate, as a metallic layer forms between them. At the percolation threshold, conductivity increases dramatically by several orders of magnitude, as coalescence creates a continuous pathway for electrons throughout the network. This threshold also leads to an exponential change in the optical properties of the film, resulting in a significant phase transition. This phenomenon is crucial for the design and engineering of thin, semitransparent metal films.

13.3. Thickness Growth

For many films, the average percolation thickness ranges from 1 to 20 nm. However, this thickness is insufficient for forming dielectric quarter-wave systems or metal mirror layers. In addition to increasing thickness through further material deposition, the actual structure is influenced by four key factors.

Shadowing: Shadowing is the geometric interaction between the roughness of the growing surface and the incoming adatoms. This effect is particularly pronounced at lower substrate temperatures (TSs), as the vapor beam is directed more effectively under these conditions.

Surface Dispersion: This refers to the mobility of adatoms along grain boundaries and other surfaces, which is most significant at medium substrate temperatures (TSs).

Bulk Diffusion: This involves the movement of adatoms within the grain volume and becomes dominant at higher temperatures.

Crystallization: This phase transition involves a complete reorientation of the crystal structure and is particularly evident at elevated substrate temperatures (TSs), greater film thicknesses, and the percolation threshold.

14. Thin-Film Sensor Application

14.1. Electrochemical Sensing

Several factors contribute to the potential of metal oxide materials in applications: (1) they can enhance the durability of films over time by increasing their chemical stability,

(2) their semiconducting properties can facilitate faster charge-transfer processes, and (3) many of these materials possess inherent catalytic activity.

Extensive research has focused on optimizing the active layers on electrodes to enhance the long-term durability, sensitivity, and selectivity of electrochemical sensors and biosensors. The chemical approach to nanotechnology, which employs bottom-up synthetic methods to create nanostructured materials on electrode surfaces, has significantly advanced this field (Table 2). A variety of metal oxides produced via sol–gel processes, including CeO_2, WO_3, ZnO, Nb_2O_5, SnO_2, MnO_2, Cu_2O, and TiO_2, have been deposited as thin films on electrode surfaces. These materials are commonly utilized as solid electrolytes or active layers in applications such as dye-sensitized solar cells, electrochromic smart windows, and energy storage devices. As will be discussed briefly below, their use in electroanalytical applications is on the rise. High concentrations of heme proteins have been successfully immobilized using mesoporous films of TiO_2, WO_3, Nb_2O_5, and Al_2O_3, serving as effective matrices that preserve the structure and activity of the biomolecules. In each case, the proteins exhibited direct electrochemistry, enabling the electrocatalytic detection of substances such as hydrogen peroxide, nitrite, and nitric oxide. It has also been noted that the semiconducting properties of materials like WO_3 and Nb_2O_5 facilitate direct electron transfer in redox proteins, eliminating the need for an additional mediator [160–163].

After the neurotransmitter catechol was adsorbed onto mesostructured TiO_2 sheets on sonogel carbon electrodes, it was detected using voltammetric methods. The sensor's strong performance was attributed to the ability of TiO_2 to facilitate charge-transfer processes and its effectiveness in detecting catechol even in the presence of common interferents such as ascorbic acid and acetaminophen. Additionally, it was found that the conductivity of mesostructured SnO_2 films was highly responsive to molecular hydrogen and adsorbed ethanol, leading to the development of selective sensors for both gases. The devices' exceptional sensitivity was credited to the large specific surface areas of the mesostructured sensing elements [164,165].

Table 2. Overview of hybrid thin-film-based sensors for applications in biology, electrochemistry, electrocatalysis, optics, and QCM [166].

Thin-Film Materials	Synthesis Route	Sensing Element
P_3HT-ZnO	Spraying	FA
PPyxMoO_3	Ex situ intercalation	FA
2DOM-Ag thin film	Nanosphere lithography at solution surface	4-amino thiophenol Avidine
(PTHNA)xMoO_3	Solution method	FA (400 ppb)
PTP/WO_3	PTP: chemical oxidative polymerization	NO_2
CNTs/rG film	Co-polymerization and vertical deposition	NO_2 (60 min)
SWCNT/TiOx/ZnO	Arc discharge	H_2 (1000 ppm)
CeO_2-ZnO	Co-evaporation	CO
Ppy-NiO	Spin coating	NO_2 (100 ppm)
Pd-PMMA	Spin coating	H_2
PDDA/MWCNT)$_6$/Ag/NPs	Layer by layer	H_2O_2
(TiO_2/PAA400)5	Gas-phase sol–gel	Ammonia
Ti(O-nBu)41 mM	Dip-coating method	Ammonia
$Zn_{Pctamyl}$	--	Methanol
$Cu^{Ptphen+}$	--	Methanol
GC-Nf-CNT-DHB	Electrochemical	NADH
$Zn^{Pctamyl}$	--	Ethanol

Nanostructured organic polymer films can be produced by electrodepositing a lyotropic liquid crystalline phase. This technique has been used to create ordered mesoporous polyaniline deposits for hydrogen peroxide sensing, enabling the immobilization of horseradish peroxidase (HRP). The resulting biosensor benefits from the large surface area of the ordered film, allowing for high HRP loading, while the strong conductivity of polyaniline facilitates efficient electron transport between HRP and the electrode. Additionally, lipid cubic phases that form a three-dimensional, well-ordered porous structure—interwoven with aqueous channels—have been identified as promising systems. These structures can enhance the mass transport of small molecules and effectively incorporate and stabilize biomolecules [167,168]. It may be surprising that continuous mesoporous carbon films utilizing silica templates have not yet been employed in electrochemical sensing, despite their outstanding electrical conductivity and very high specific surface areas. To date, research has focused on composite films made from ordered mesoporous carbon (OMC) particles incorporated into an organic polymer matrix. These composite films have been used to detect redox-active analytes. For instance, a glassy carbon electrode modified with OMC–Nafion was reported to enable the sensitive detection of L-cysteine, achieving the lowest limit of detection (LOD) ever noted for the direct measurement of this compound, at just 2 nM [169].

14.2. Gas Sensors

Mesoporous silica thin films, deposited via evaporation-induced self-assembly (EISA) on interdigitated electrodes, have been employed to develop gas sensors that exhibited a rapid resistive response to fluctuations in relative humidity and alcohol vapors. The changes in conductivity during gas adsorption drive the electrode's response. The overall performance of the sensor is significantly affected by the composition of the surfactant template used [170,171].

14.3. Biosensors

Biosensors that incorporate proteins immobilized in silica films are starting to gain attention, with the primary aim being to facilitate the direct electrochemistry of biomolecules, as recently illustrated with hemoglobin reactions [172]. This research has expanded to include other proteins, such as cytochrome C [173] and glucose oxidase [174], focusing on mesoporous silica particles that contain these enzymes [175] or heme proteins. The motivation behind these strategies lies in the appealing hosting properties of mesostructured materials, which are believed to create an ideal environment for biomolecular activity through a mild encapsulation method. Additionally, a thorough review of the various techniques for immobilizing enzymes on ordered mesoporous materials has been conducted to enhance understanding and improve sensor functionality.

14.4. Electrocatalytic Devices

Although mesoporous materials hold great promise as host materials for various catalysts, their use has not become as widespread as anticipated. When nicotinamide adenine dinucleotide (NAD^+) is encapsulated in mesoporous silicates, it exhibits significant electrocatalytic activity for the oxidation of 1,4-dihydrobenzoquinone. Additionally, the incorporation of gold nanoparticles onto amine-functionalized mesoporous silica sheets has been shown to significantly enhance the catalysis of glucose oxidation [176,177].

15. Preconcentration Electroanalysis

This process involves attaching selective recognition elements to (often functionalized) mesoporous silica film, allowing the target analyte to accumulate at open-circuit conditions before being detected voltammetrically on the electrode surface. Detection of metals such

as Pb^{2+} is typically performed using anodic stripping voltammetry in square wave or differential pulse modes [178,179]. For instance, thiol-functionalized mesoporous silica has been deposited on gold electrode arrays and glassy carbon electrodes for this purpose. Additionally, oriented amine-functionalized silica films have been utilized for the detection of Cu^{2+}. The sensitivity of the sensor was found to be closely related to the degree of three-dimensional organization in the film and the quantity of organo-functional groups present. This is because the diffusion of target analytes toward the binding sites within the mesoporous film is the rate-determining step. Additionally, functionalized porous clay heterostructures, which feature well-ordered mesopore channels in the interlayer region of the clay, are of particular interest. These structures have the potential to form macro-mesoporous films on electrode surfaces, which are expected to enhance sensitivity in preconcentration electroanalysis [180].

16. Prospective Developments in Thin-Film Sensing and Thin-Film Materials

Recent years have seen significant advancements in the creation of highly ordered porous structures on various solid supports, including electrodes. Both sol–gel-derived mesoporous metal oxides and macroporous conductive materials have been successfully produced. Currently, the use of molecular or particle assemblies as templates enables greater control over the final porosity structure, pore size, and level of interconnectivity. The primary advantage of these nanoengineered materials lies in their exceptionally large surface areas, which can be several orders of magnitude greater than the geometric area of the underlying electrode. These expansive surface areas are anticipated to enhance exposure to solutions and create optimal conditions for the functionalization or immobilization of reagents. Furthermore, in electrochemical sensing applications, the uniform spatial arrangement across extensive areas guarantees strong connectivity among the pores, leading to rapid mass transfer rates and heightened sensitivity. Although electroanalysis is still an emerging field, there are several applications. These largely revolve around the immobilization of appropriate reagents or biomolecules, which are utilized for the selective and sensitive detection of target analytes, particularly contaminants or biologically relevant species. Furthermore, in electrochemical sensing applications, the uniform spatial arrangement across extensive areas guarantees strong connectivity among the pores, leading to rapid mass transfer rates and heightened sensitivity. Although electroanalysis is still an emerging field, there are several applications. These largely revolve around the immobilization of appropriate reagents or biomolecules, which are utilized for the selective and sensitive detection of target analytes, particularly contaminants or biologically relevant species. The development of mesostructured deposits from sol–gel processes on the internal surfaces of conductive macroporous electrodes presents an intriguing opportunity. Continued research could result in a novel class of nanomaterials that leverage the rich chemistry of organic–inorganic hybrids based on silica, along with the exceptionally high active surface areas of porous, ordered metal electrodes. There remains significant potential to enhance the selectivity of recognition events, even though some pre-concentration features of sensitive layers have already been successfully implemented. Achieving this would require the use of highly porous materials with effective pore interconnectivity to construct more complex, integrated chemical systems. This could involve immobilizing macrocyclic ligands or creating structured configurations of enzymes, cofactors, and mediators. Enhancing the long-term and operational stability of these ordered porous layers, particularly those derived from sol–gel materials, will necessitate exploring metal oxides beyond silica and seeking ways to functionalize their internal structures. While silica offers rich chemistry, its stability in aqueous environments can be lacking. In contrast, some

other metal oxides exhibit greater chemical stability but may pose challenges in terms of functionalizing with organic groups. Attempts to address these issues would greatly benefit from close collaboration among materials scientists, organic chemists, biologists, and electrochemists. We also anticipate that such devices could find applications in various fields that require large surface areas, rapid mass transfer, high conductivity, or effective hosting properties, including power sources, photovoltaic devices, separation technologies, reactive membranes, and catalytically active materials [181–184].

This paper offers a concise summary of thin-film deposition, the importance and significance of the thin-film growth process, and its applications. To improve the techniques of the thin-film deposition process, further research is needed on the use of computer simulation models, which are increasingly valuable for controlled thin-film operations. The theoretical study will focus on controlling the growth and adhesion of electrodeposited films used in devices. Furthermore, these models will be applied to enhance the control of nanostructured film layers. Moreover, environmentally friendly flexible electronics will use biodegradable cellulose nanofibril paper. Such advancements result in high-performance, versatile, and eco-friendly devices. Therefore, future research should focus on reducing sintering temperatures and production costs, improving thin-film quality, and developing environmentally safe thin films. This will expand the potential applications of conductive thin films [185,186].

17. Electrochemistry of Thin-Film Materials

Electrochemistry provides simple methods for producing a range of thin films and nanostructured materials. On the other hand, analytical instruments for the electrochemical characterization, functionalization, and modification of new thin-film materials are employed to identify and detect different analytes. Electrochemical methods are simple, cost-effective, and do not require expensive, specialized equipment, making thin films suitable for any research lab. Thin-film materials can be efficiently produced using both cathodic reduction and anodic oxidation electrochemical techniques [166].

17.1. Synthesis of Thin-Film Materials Through Cathodic Processes

Cathodic deposition in various modes, such as constant current density, constant potential, pulsed electrodeposition, or cyclic voltammetry (CV), allows for the easy creation of a wide range of metals, alloys, metal oxides, and thin films. It is important to note that the potentiostatic mode employs a three-electrode cell, while the galvanostatic mode uses a two-electrode setup. The characteristics of the deposit, including its chemical composition, homogeneity, thickness, and microstructure, are affected by cathodic deposition parameters such as electrolyte composition, temperature, deposition time, electrolyte agitation, and the applied current/potential. One of the advantages of the cathodic deposition of various materials is the ability to control the crystal nucleation and growth process by adjusting factors such as additives, ion concentration in the solution, and the applied current density/potential. Metal alloys and composite materials can be deposited, provided their reduction potentials are close enough to each other. The deposition is performed directly onto the conducting substrate. It is well established that metals can be catholically electrodeposited from solutions as coatings and thin films. These techniques have been studied and improved over many years to create protective and decorative coatings on various substrates. It is widely recognized that specific additives in the electrolyte used for electrodeposition can accelerate the formation of metal layers. Since the findings can be applied to the copper electrorefining process, understanding the effect of various compounds present in the electrolyte on the kinetics and mechanism of electrochemical copper deposition could be of considerable practical importance. Rendón-Enríquez et al. introduced a

reductive electrochemical method for the cyclic voltammetry deposition of polymer films using 1,3,5-tris (2-chloropyrid-5-yl) benzene and 1,3,5-tris(2-bromopyrid-5-yl) benzene monomers dissolved in dimethylformamide (DMF) [26,187].

The deposition took place on ITO substrates or platinum-coated quartz crystals. These polymer thin films are attractive for potential applications in photovoltaic or photogalvanic cells. According to the Ropero-Vega et al.'s study, Au nanoparticles (NPs) can be deposited onto screen-printed electrodes for possible use in electrochemical biosensors to detect *Escherichia coli* in aqueous environments. The morphology of AuNPs deposited on the electrode surface was studied in relation to the applied voltage (ranging from 0.05 V to −0.25 V vs. Ag/AgCl) and the deposition time (20–250 s). The AuNPs were electrode-deposited in a solution of 1.0 mM $HAuCl_4$ and 0.5 M H_2SO_4 at a constant potential. In these studies, the conditions for the electrochemical cathodic deposition of AuNPs on the electrode surface (−0.05 V vs. Ag/AgCl and 100 s) were optimized. Cathodic methods are commonly used to produce nanostructured materials, including metallic, composite, semiconductor, and other nanoparticles and nanowires [188].

17.2. Synthesis of Thin-Film Materials Through Anodic Processes

Anodic oxidation is the most widely used and cost-effective method for producing thin oxide coatings on metals or conductive polymers across various substrates. For over a century, aluminum and its alloys have been coated with decorative and protective layers formed through the anodic oxidation of metals. The introduction of the two-step anodizing process by Masuda and Satoh in 1996, which produced densely packed and highly organized nanoporous aluminum oxide layers, marked a significant breakthrough that enabled the use of anodic aluminum oxide (AAO) in nanotechnology. Since then, there have been significant advancements in the characterization, application, and anodic oxidation of aluminum. Anodizing conditions, such as electrolyte type and composition, applied voltage, electrolyte temperature, and duration, easily control the structural properties of nanoporous AAO, including pore diameter, interpore distance, layer thickness, pore density, and porosity. In recent years, anodization has also been adapted for creating nanoporous/nanotubular oxide layers on the surfaces of various metals, including Ti, W, Sn, Zn, Hf, Nb, Zr, and Mo. Husak et al. explored the plasma electrolytic oxidation of pure magnesium in different silicate-based solutions, which contained varying amounts of calcium hydroxide, sodium hydroxide, sodium silicate, and sodium fluoride. A potential of 200–300 V was applied for 10 min to form a ceramic layer on the magnesium surface. The corrosion properties of the new coatings were then studied through extended immersion in simulated body fluid [189,190].

17.3. Electrochemical Characterization of Thin-Film Materials

Electrochemical techniques have been used for many years to study various materials and electrodes, as they provide valuable insights across a range of application areas. Potential sweep methods, especially linear sweep and cyclic voltammetry (LSV and CV), are commonly used as simple, versatile techniques to characterize the redox properties of molecules and examine the kinetics of various electrode processes occurring on the surface of the materials or electrodes being tested. Step techniques (such as chronoamperometry and chronopotentiometry) and pulse voltammetric methods (including differential pulse voltammetry, normal pulse voltammetry, and square wave voltammetry) are also commonly used electrochemical techniques in the fields of electrochemistry and electroanalysis. Electrochemical impedance spectroscopy (EIS) is a non-destructive technique that can also be applied to investigate various electrochemical systems and processes. Its applications span across corrosion, thin-film and coating characterization, batteries, semiconductor

electrodes, sensors, biological systems, and more. It allows for the analysis of bulk and interfacial processes, with time constants ranging from minutes to microseconds. It is essential to highlight that electrochemical experiments are usually conducted with a substantial excess of supporting electrolytes to ensure that the electrolyte ions carry charge in the solution. In contrast, the migration of charged reactants and products can be disregarded under these conditions [191,192].

18. Thin-Film Growth of MAX Phases

Layered nanolaminate ternary carbides and nitrides, with the chemical formula $M_{n+1}AX_n$ or MAX (where n = 1, 2, or 3, M is an early-transition metal, A is a group 13 or 14 element, and X is C and/or N), represent a unique class of materials that combine both ceramic and metallic properties. The remarkable mechanical properties of nanolaminate MAX materials such as their high hardness, low friction coefficient, excellent oxidation resistance, superior damage tolerance compared to that of other ceramics, high corrosion, thermal shock resistance, strong radiation damage tolerance for space and nuclear applications, and high electrical and thermal conductivity are all attributed to their unique structure. The discovery of the MAX phase was first reported by Nowotnys Group in 1963. The MAX phase is further categorized into the (M_2AX), (M_3AX_2), and (M_4AX_3) phases (Figure 16). It was noted that epitaxial thin films also demonstrate exceptional electrical, thermal, mechanical, tribological, magnetic, oxidation resistance, and corrosion properties. These characteristics make MAX-based devices highly promising for applications in high-temperature industrial settings, as well as in lubricant and coating materials, radiation-resistant nuclear materials, solar panels, and spacecraft [193–195].

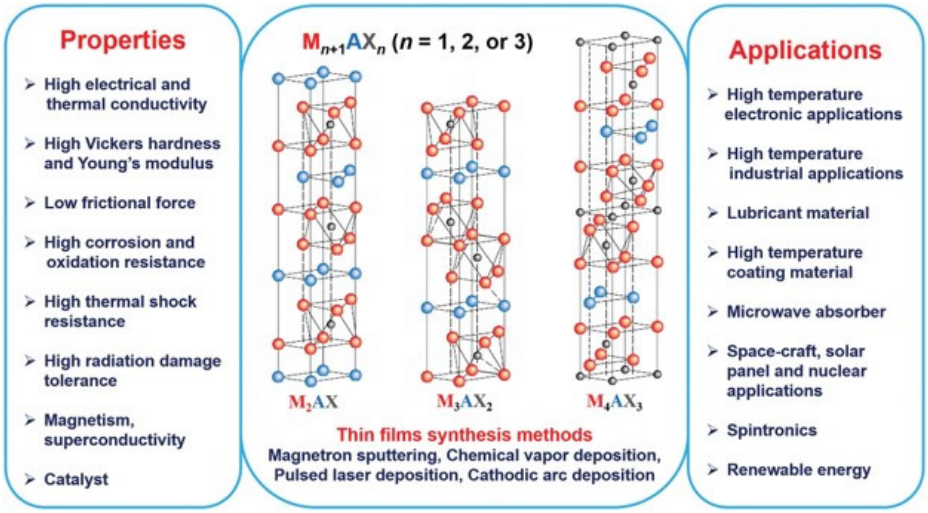

Figure 16. Layered ternary $M_{n+1}AX_n$ (n = 1–3) with a wide range of properties and applications. (Reference [195]. This is an open-access article distributed under the terms of the Creative Commons CC BY license.)

MAX Phase Thin Films

The first multilayer compound in the ternary MAX series demonstrates excellent metallic properties and remarkable durability in harsh conditions, including high temperatures, corrosive environments, and oxidizing environments. The material exhibits significant anisotropy due to its large lattice constant ratio. A typical band structure calculation shows that the Ti-3d orbitals contribute most of the charge carriers (p-type), and there is a considerable density of states (DOS) at the Fermi level (EF). As a result, the material synthesis community recognized the production of thin films of 211 MAX phases as an intriguing approach [196,197]. Wilhelmsson et al. were the first to report the epitaxial growth of

Ti_2AlC MAX phase thin films using the magnetron sputtering deposition process. Rosen et al. used high-resolution HRTEM to grow epitaxial Ti_2AlC thin films on sapphire and identified an epitaxial relationship between (001) (Ti_2AlC)//(0001) (Al_2O_3) and (11-20) (Ti_2AlC)//(11-20) (Al_2O_3). In addition, Pshyk et al. employed electron beam physical vapor deposition at 700 °C to grow 120 nm Ti_2AlC MAX phase thin films. They subsequently analyzed the material structural, nano-mechanical, and tribological properties, finding that their hardness and elastic modulus were 4.8 and 182.5 GPa, respectively. Frodelius et al. found that additional Ti flux is required to produce the stoichiometric 211 MAX phase after they attempted to optimize the growth of the Ti_2AlC phase through sputtering. Furthermore, Feng et al. found that the formation of high-quality Ti_2AlC-phase thin films relies on high-temperature annealing. Using the magnetron sputtering method, Högberg et al. reported the growth of epitaxial Ti_2GeC thin films on Al_2O_3 (0001) substrates at 1000 °C. Further, Emmerlich et al. reported the development of Ti_2GeC and Ti_2SnC thin films with low electrical resistivity, ranging from 15 to 50 μΩ·cm. Beckers et al. employed reactive sputtering techniques to grow Ti_2AlN films on MgO (111) and Al_2O_3 (0001) substrates. They found that the film deteriorates around 800 °C due to the subsequent diffusion of Al. Moreover, the Nb_2AlC thin film produced by Scabarozi et al. on sapphire using magnetron sputtering notably exhibits a superconducting transition at 440 mK. After that, Hopfeld et al. measured the tribological properties of Cr_2AlC films and found that the friction coefficients ranged from 0.30 to 0.70. Also, Jiang et al. tried to produce V_2AlC thin films using magnetron sputtering. Dahlqvist et al. investigated the magnetic properties of Mn_2GaC thin films grown on MgO (111) substrates. They discovered ferromagnetic ordering and magnetically induced anisotropic structural changes below 230 K, as well as strong intralayer ferromagnetic spin coupling. HRTEM analysis confirmed that a (Ti, Zr)$_2$AlC solid solution MAX phase film was formed when Azina et al. sputtered a (Ti, Zr)$_2$AlC target onto an Al_2O_3 (0001) substrate. Moreover, Mockute et al. employed sputtering to produce nanolaminate (Cr, Mn)$_2$AlC thin films on Al_2O_3 (0001). Meshkian et al. produced high-quality $(Mo_{0.5}Mn_{0.5})_2GaC$ thin films on MgO (111) substrates, and magnetic testing showed a remanent magnetization (Mr) of 0.35 μB/atom at low temperature, indicating ferromagnetism. Subsequently, Petruhins et al. grew $(Cr_{0.5}Mn_{0.5})_2GaC$ films on MgO (111), 4H-SiC (0001), and Al_2O_3 (0001) substrates, both with and without a NbN (111) seed layer. At 30 K and under a magnetic field of 5 Tesla, they observed a net magnetic moment of 0.67 μB/(Cr + Mn) atom. Moreover, the ferromagnetic resonance spectra of the same film, measured by Salikhov et al., showed minimal magneto-crystalline anisotropy [198–201].

19. Summary of This Review

This review article discusses the recent advances and achievements in the field of thin-film technology over the last two decades. The discussion covers the various substrates used in the production of thin films. Additionally, the different thin-film fabrication methods and techniques are explained, such as chemical vapor deposition, thermal evaporation, sputtering, gas-phase fabrication, liquid-phase fabrication, electrochemical deposition, electrospinning, glancing angle deposition, and chemical precipitation. Several types of thin-film applications, including those for biomedical sensors, chemical sensors, temperature sensors, force sensors, pressure sensors, humidity sensors, strain sensors, biomedical applications, corrosion applications, optical applications, energy applications, and antimicrobial properties, are also discussed. A variety of techniques for characterizing the properties of thin-film devices and prospective developments in thin-film technology are explored.

Author Contributions: Conceptualization, S.S., G.A.M., S.V., C.-L.Y., C.-L.C. and T.-W.C.; writing—original draft preparation, S.S., G.A.M., S.V., C.-L.Y., C.-L.C., T.-W.C. and N.V.; writing—review and editing, S.S., G.A.M., S.V., C.-L.Y., C.-L.C. and T.-W.C.; project administration, S.S. and T.-W.C.; visualization, S.S., G.A.M. and N.V.; supervision, S.S., C.-L.C. and T.-W.C. All authors have read and agreed to the published version of the manuscript.

Funding: This research was funded by National Science and Technology Council, Taiwan, grant number NSTC 113-2221-E- 027-033-, NSTC 112-2221-E-027-039-, and NSTC 112-2221-E-027-032) and the National Taipei University of Technology–King Mongkut's Institute of Technology Ladkrabang Joint Research Program (NTUT-KMITL-113-01).

Data Availability Statement: Data will be made available upon request.

Acknowledgments: We acknowledge the National Science and Technology Council Taiwan and The National Taipei University of Technology–King Mongkut's Institute of Technology, Ladkrabang Joint Research Program.

Conflicts of Interest: The authors declare no conflicts of interest.

References

1. Abou-Ras, D.; Kirchartz, T.; Rau, U. (Eds.) *Advanced Characterization Techniques for Thin Film Solar Cells*; Wiley-VCH Verlag GmbH & Co. KGaA: Weinheim, Germany, 2016.
2. Raut, H.K.; Ganesh, V.A.; Nair, A.S.; Ramakrishna, S. Anti-reflective coatings: A critical, in-depth review. *Energy Environ. Sci.* **2011**, *4*, 3779. [CrossRef]
3. McDonnell, S.J.; Wallace, R.M. Atomically-thin layered films for device applications based upon 2DTMDC materials. *Thin Solid Films* **2016**, *616*, 482–501. [CrossRef]
4. Lee, S.D.; Lee, Y.J.; Nam, K.S.; Jeong, Y.; Kim, D.H.; Kim, C.S.; Park, S.G.; Kwon, S.H.; Kwon, J.D.; Park, J.S. Characterization of microcrystalline silicon thin film solar cells prepared by high working pressure plasma-enhanced chemical vapor deposition. *J. Electroceramics* **2014**, *33*, 149–154. [CrossRef]
5. Khan, H.F.H.R. *Handbook of Thin-Film Technology*; Springer: Berlin/Heidelberg, Germany, 2015; ISBN 978-3-642-05429-7. [CrossRef]
6. Chiu, T.W.; Wakiya, N.; Shinozaki, K.; Mizutani, N. Effect of substrate size on crystalline Orientation and Electrical Properties of $(Bi, La)_4Ti_3O_{12}$ Thin Films. *J. Ceram. Soc. Jpn.* **2004**, *112*, 266–270. [CrossRef]
7. Chiu, T.W.; Tonooka, K.; Kikuchi, N. Growth of b-axis oriented VO_2 thin films on glass substrates using ZnO buffer layer. *Appl. Surf. Sci.* **2010**, *256*, 6834–6837. [CrossRef]
8. Chiu, T.W.; Wakiya, N.; Shinozaki, K.; Mizutani, N. Growth of highly (001)-textured strontium barium niobate thin films on epitaxial $LaNiO_3/CeO_2/YSZ/Si(100)$. *Thin Solid Films* **2003**, *426*, 62–67. [CrossRef]
9. Chiu, T.W.; Hong, R.T.; Tonooka, K.; Kikuchi, N. Microstructure of orientation controlled VO_2 thin films via ZnO buffer. *Thin Solid Films* **2013**, *529*, 119–122. [CrossRef]
10. Chiu, T.W.; Tanabe, M.; Uedono, A.; Hasunuma, R.; Yamabe, K. Study of Interactions of Hf and SiO_2 Film for High-k Materials. *Jpn. J. Appl. Phys.* **2006**, *45*, 6253–6255. [CrossRef]
11. Cranston, R.R.; Lessard, B.H. Metal phthalocyanines: Thin-film formation, microstructure, and physical properties. *RSC Adv.* **2021**, *11*, 21716–21737. [CrossRef]
12. Elanjeitsenni, V.P.; Vadivu, K.S.; Prasanth, B.M. A review on thin films, conducting polymers as sensor devices. *Mater. Res. Express* **2022**, *9*, 022001. [CrossRef]
13. Chiu, T.W.; Wakiya, N.; Shinozaki, K.; Mizutani, N. Electrical properties of vanadium doped Bi-LaTi-O thin films derived by chemical solution deposition method. *Integr. Ferroelectr.* **2002**, *47*, 187–196. [CrossRef]
14. Chiu, T.W.; Shih, J.H.; Chang, C.H. Preparation and properties of $CuCr_{1-x}Fe_xO_2$ thin films prepared by chemical solution deposition with two-step annealing. *Thin Solid Films* **2016**, *618*, 151–158. [CrossRef]
15. Chiu, T.W.; Tsai, S.W.; Wang, Y.P.; Hsu, K.H. Preparation of p-type conductive transparent $CuCrO_2$:Mg thin films by chemical solution deposition with two-step annealing. *Ceram. Int.* **2012**, *38* (Suppl. S1), S673–S676. [CrossRef]
16. Forgerini, F.L.; Marchiori, R. A brief review of mathematical models of thin film growth and surfaces. *Biomatter* **2014**, *4*, e28871. [CrossRef]
17. Zhang, Z.; Lagally, M.G. Atomistic processes in the early stages of thin-film growth. *Science* **1997**, *276*, 377–383. [CrossRef] [PubMed]
18. Budida, J.; Srinivasan, K. Review of thin film deposition and techniques. *Mater. Today Proc.* **2023**, *92*, 1030–1033. [CrossRef]

19. Gilmer, G.H.; Huang, H.; Roland, C. Thin film deposition: Fundamentals and modeling. *Comput. Mater. Sci.* **1998**, *12*, 354–380. [CrossRef]
20. Workie, A.B.; Ningsih, H.S.; Shih, S.J. An comprehensive review on the spray pyrolysis technique: Historical context, operational factors, classifications, and product applications. *J. Anal. Appl. Pyrol.* **2023**, *170*, 105915. [CrossRef]
21. Rossnagel, S.M. Thin film deposition with physical vapor deposition and related technologies. *J. Vac. Sci. Technol. A* **2003**, *21*, S74–S87. [CrossRef]
22. Chen, X.; Dai, W.; Wu, T.; Luo, W.; Yang, J.; Jiang, W.; Wang, L. Thin film thermoelectric materials: Classification, characterization, and potential for wearable applications. *Coatings* **2018**, *8*, 244. [CrossRef]
23. Lee, S.D.; Nam, S.H.; Kim, M.H.; Boo, J.H. Synthesis and Photocatalytic Property of ZnO nanoparticles Prepared by Spray-Pyrolysis Method. *Phys. Procedia* **2012**, *32*, 320–326. [CrossRef]
24. Kunene, T.J.; Tartibu, L.K.; Ukoba, K.; Jen, T.C. Review of atomic layer deposition process, application and modeling tools. *Mater. Today Proc.* **2022**, *62*, S95–S109. [CrossRef]
25. Gaspari, F. Thin Films. *Compr. Energy Syst.* **2018**, *2*, 88–116. [CrossRef]
26. Pedersen, H.; Barry, S.T.; Sundqvist, J. Green CVD Toward a sustainable philosophy for thin film deposition by chemical vapor deposition. *J. Vac. Sci. Technol. A.* **2021**, *39*, 051001. [CrossRef]
27. Maruyama, T.; Arai, S. Titanium dioxide thin films prepared by chemical vapor deposition. *Sol. Energy Mater. Sol. Cells* **1992**, *26*, 323–329. [CrossRef]
28. Wang, Y.; Lu, D.; Wang, F.; Zhang, D.; Zhong, J.; Liang, B.; Gui, X.; Sun, L. A new strategy to prepare carbon nanotube thin film by the combination of top-down and bottom-up approaches. *Carbon* **2020**, *161*, 563–569. [CrossRef]
29. Shah, A. *Thin-Film Silicon Solar Cells*; CRC Press: Boca Raton, FL, USA, 2010.
30. Jones, A.C.; Hitchman, M.L. *Chemical Vapour Deposition: Precursors, Processes and Applications*; RSC Publishing: London, UK, 2009.
31. Morosanu, C.E.; Siddall, G. *Thin Films by Chemical Vapour Deposition*; Elsevier: Amsterdam, The Netherlands, 1990. [CrossRef]
32. Venables, J. *Introduction to Surfaces and Thin Film Processes*; Cambridge University Press: Cambridge, UK, 2000.
33. Revathi, N.; Bereznev, S.; Loorits, M.; Raudoja, J.; Lehner, J.; Gurevits, J.; Traksmaa, R.; Mikli, V.; Mellikov, E.; Volobujeva, O. Annealing effect for SnS thin films prepared by high-vacuum evaporation. *J. Vac. Sci. Technol. A* **2014**, *32*, 061506. [CrossRef]
34. Safarian, J.; Engh, T.A. Vacuum evaporation of pure metals. *Metall. Mater. Trans. A* **2013**, *44*, 747–753. [CrossRef]
35. Tan, H.W.; An, J.; Chua, C.K.; Tran, T. Metallic nanoparticle inks for 3D printing of electronics. *Adv. Electron. Mater.* **2019**, *5*, 1800831. [CrossRef]
36. Liu, J.; Li, X.; Zeng, X. Silver nanoparticles prepared by chemical reduction-protection method, and their application in electrically conductive silver nanopaste. *J. Alloys Compd.* **2010**, *494*, 84–87. [CrossRef]
37. Pudas, M.; Halonen, N.; Granat, P.; Vahakangas, J. Gravure printing of conductive particulate polymer inks on flexible substrates. *Prog. Org. Coat.* **2005**, *54*, 310–316. [CrossRef]
38. Chen, S.P.; Liao, Y.C. Highly stretchable and conductive silver nanowire thin films formed by soldering nano mesh junctions. *Phys. Chem. Chem. Phys.* **2014**, *16*, 19856–19860. [CrossRef] [PubMed]
39. Li, B.; Liu, Q.; Zhang, Y.; Liu, Z.; Geng, L. Highly conductive Nb doped $BaSnO_3$ thin films on MgO substrates by pulsed laser deposition. *J. Alloys Compd.* **2016**, *680*, 343–349. [CrossRef]
40. Kikuchi, N.; Komatsu, T.; Yoshimura, H. Characteristics of thin film growth in the synthesis of diamond by chemical vapour deposition and application of the thin film synthesis technology for tools. *Mater. Sci. Eng. A* **1988**, *105*, 525–534. [CrossRef]
41. George, S.M. Atomic layer deposition: An overview. *Chem. Rev.* **2009**, *110*, 111–131. [CrossRef]
42. Sun, L.; Yuan, G.; Gao, L.; Yang, J.; Chhowalla, M.; Gharahcheshmeh, M.H.; Gleason, K.K.; Choi, Y.S.; Hong, B.H.; Liu, Z. Chemical vapour deposition. *Nat. Rev. Methods Primers* **2021**, *1*, 5. [CrossRef]
43. Hitchman, M.L.; Tian, F. Studies of TiO_2 thin films prepared by chemical vapor deposition for photocatalytic and photo electrocatalytic degradation of 4-chlorophenol. *J. Electroanal. Chem.* **2002**, *538*, 165–172. [CrossRef]
44. Maruyama, T. Copper oxide thin films prepared by chemical vapor deposition from copper dipivaloyl methanate. *Sol. Energy Mater. Sol. Cells* **1998**, *56*, 85–92. [CrossRef]
45. Fouad, O.A.; Ismail, A.A.; Zaki, Z.I.; Mohamed, R.M. Zinc oxide thin films prepared by thermal evaporation deposition and its photocatalytic activity. *Appl. Catal. B Environ.* **2006**, *62*, 144–149. [CrossRef]
46. Hasim, S.N.F.; Hamid, M.A.A.; Shamsudin, R.; Jalar, A. Synthesis and characterization of ZnO thin films by thermal evaporation. *J. Phys. Chem. Solids* **2009**, *70*, 1501–1504. [CrossRef]
47. Chiu, T.W.; Yang, Y.C.; Yeh, A.C.; Wang, Y.P.; Feng, Y.W. Antibacterial property of $CuCrO_2$ thin films prepared by RF magnetron sputtering deposition. *Vacuum* **2013**, *87*, 174–177. [CrossRef]
48. Chen, L.F.; Wang, Y.P.; Chiu, T.W.; Shih, W.C.; Wu, M.S. Fabrication of transparent $CuCrO_2$:Mg/ZnO p–n junctions prepared by magnetron sputtering on an indium tin oxide glass substrate. *Jpn. J. Appl. Phys.* **2013**, *52*, 05EC02. [CrossRef]
49. Chiu, T.W.; Chang, C.H.; Yang, L.W.; Wang, Y.P. Preparation of transparent $Cu_2Y_2O_5$ thin films by RF magnetron sputtering. *Appl. Surf. Sci.* **2015**, *354*, 110. [CrossRef]

50. Yang, T.C.K.; Yang, Y.L.; Juang, R.C.; Chiu, T.W.; Chen, C.C. The novel preparation method of high-performance thermochromic vanadium dioxide thin films by thermal oxidation of vanadium stainless steel co-sputtered films. *Vacuum* **2015**, *121*, 310–316. [CrossRef]
51. Pakpum, C. Preparation of copper thin film mask by sputtering technique assisted by polymer mask photolithography. *IOP Conf. Ser. Mater. Sci. Eng.* **2017**, *213*, 012023. [CrossRef]
52. Garg, R.; Gonuguntla, S.; Saddam, S.K.; Iqbal, M.S.; Dada, A.O.; Pal, U.; Ahmadipour, M. Sputtering thin films: Materials, applications, challenges and future directions. *Adv. Colloid Interface Sci.* **2024**, *330*, 103203. [CrossRef]
53. Thabit, N.Y.A.; Makhlouf, A.S.H. Chapter 1-Fundamental of smart coatings and thin films: Synthesis, deposition methods, and industrial applications. In *Advances in Smart Coatings and Thin Films for Future Industrial and Biomedical Engineering Applications*; Elsevier: Amsterdam, The Netherlands, 2020; pp. 3–35.
54. Stoian, M.; Maurer, T.; Lamri, S.; Fechete, I. Techniques of preparation of thin films: Catalytic combustion. *Catalysts* **2021**, *11*, 1530. [CrossRef]
55. Eckertova, L. Methods of preparation of thin films. In *Physics of Thin Films*; Springer: Boston, MA, USA, 1977. [CrossRef]
56. Reichelt, K.; Jiang, X. The preparation of thin films by physical vapour deposition methods. *Thin Solid Films* **1990**, *191*, 91–126. [CrossRef]
57. Hudandini, M.; Kusdianto, K.; Kubo, M.; Shimada, M. Gas-phase fabrication and photocatalytic activity of TiO_2 and TiO_2–CuO nanoparticulate thin films. *Materials* **2024**, *17*, 1149. [CrossRef]
58. Crivello, C.; Sevim, S.; Graniel, O.; Franco, C.; Pane, S.; Luis, J.P.; Rojas, D.M. Advanced technologies for the fabrication of MOF thin films. *Mater. Horiz.* **2021**, *8*, 168–178. [CrossRef]
59. Jeong, H.; Park, G.; Jeon, J.; Park, S.S. Fabricating large-area thin films of 2D conductive metal organic frameworks. *Acc. Chem. Res.* **2024**, *57*, 2336–2346. [CrossRef]
60. Chernikova, V.; Shekhah, O.; Eddaoudi, M. Advanced fabrication method for the preparation of MOF thin films:Liquid phase epitaxy approach meets spin coating method. *ACS Appl. Mater. Interfaces* **2016**, *8*, 20459–20464. [CrossRef]
61. Werta, S.Z.; Echendu, O.K.; Egbo, K.O.; Dejene, F.B. Electrochemical deposition and characterization of thin-film $Cd_{1-x}Zn_xS$ for solar cell application: The effect of cathodic deposition voltage. *Thin Solid Films* **2019**, *689*, 137511. [CrossRef]
62. Juarez, M.D.L.G.; Flores, E.; Gonzalez, M.M.; Nandhakumar, I.; Bradshaw, D. Electrochemical deposition and thermoelectric characterization of a semiconducting 2-D metal organic framework thin film. *J. Mater. Chem. A* **2020**, *8*, 13197–13206. [CrossRef]
63. Yu, C.L.; Weng, C.H.; Huang, R.J.; Sakthinathan, S.; Chiu, T.W.; Dong, C. Preparation of $CuCrO_2$ anisotropic delafossite-type thin film by electrospinning on glass substrates. *Ceramics* **2021**, *4*, 364–377. [CrossRef]
64. Feng, C.; Zhang, W.; Wang, J.; Zhao, Y.; Yi, K.; Shao, J. High performance of broadband anti-reflection film by glancing angle deposition. *Opt. Mater. Express* **2022**, *12*, 2226. [CrossRef]
65. Liedtke, S.; Gruner, C.; Lotnyk, A.; Rauschenbach, B. Glancing angle deposition of sculptured thin metal films at room temperature. *Nanotechnology* **2017**, *28*, 385604. [CrossRef] [PubMed]
66. Haghighi, S.B.; Khare, C.; Trocoli, R.; Dushina, A.; Kieschnick, M.; Mantia, F.L.; Ludwig, A. Synthesis of nanostructured $LiMn_2O_4$ thin films by glancing angle deposition for Li-ion battery applications. *Nanotechnology* **2016**, *27*, 455402. [CrossRef] [PubMed]
67. Zainal, Z.; Nagalingam, S.; Loo, T.C. Copper selenide thin films prepared using combination of chemical precipitation and dip coating method. *Mater. Lett.* **2005**, *59*, 1391–1394. [CrossRef]
68. Rajendran, K.; Senthil Kumar, V.; Anitha Rani, K. Synthesis and characterization of immobilized activated carbon doped TiO_2 thin films. *Optik* **2014**, *125*, 1993–1996. [CrossRef]
69. Hobbs, S.K.; Shi, G.; Bednarski, M.D. Synthesis of polymerized thin films for immobilized ligand display in proteomic analysis. *Bioconjugate Chem.* **2003**, *14*, 526–531. [CrossRef]
70. Jiang, Y.; Liu, Z.; Zhou, H.; Sharma, A.; Deng, J.; Ke, C. Physical adsorption and oxidation of ultrathin MoS_2 crystals: Insights into surface engineering for 2D electronics and beyond. *Nanotechnology* **2023**, *34*, 405701. [CrossRef] [PubMed]
71. Ma, S.; Sui, J.; Cao, L.; Li, Y.; Dong, H.; Zhang, Q.; Dong, L. Synthesis of Cu_2ZnSnS_4 thin film through chemical successive ionic layer adsorption and reactions. *Appl. Surf. Sci.* **2015**, *349*, 430–436. [CrossRef]
72. Vankova, S.; Zanarini, S.; Amici, J.; Camara, F.; Arletti, R.; Bodoardo, S.; Penazzia, N. WO_3 nanorolls self-assembled as thin films by hydrothermal synthesis. *Nanoscale* **2015**, *7*, 7174–7177. [CrossRef]
73. Pingsheng, H.; Jianmin, B.; Gang, Y.; Guien, Z.; Changsui, W. Preparation of thin film of TS and PTS by Langmuir-Blodgett techniques. *J. Mater. Sci.* **1989**, *24*, 1901–1903. [CrossRef]
74. Gole, A.; Jana, N.R.; Selvan, S.T.; Ying, J.Y. Langmuir-blodgett thin films of quantum dots: Synthesis, surface modification, and fluorescence resonance energy transfer (FRET) studies. *Langmuir* **2008**, *24*, 8181–8186. [CrossRef] [PubMed]
75. Yu, C.L.; Sakthinathan, S.; Lu, M.T.; Yu, S.T.; Kuo, C.Y.; You, Y.F.; Chiu, T.W. $CuAlO_2$/AlN double-layer thin film prepared by the spin coating approach. *Thin Solid Films* **2022**, *753*, 139260. [CrossRef]
76. Feng, J.; Fan, J.; Zhang, Z.; Gao, Y.; Xue, S.; Cai, G.; Zhao, J.S. Spin-Coating Deposited SnS_2 Thin Film-Based Memristor for Emulating Synapses. *Adv. Funct. Mater.* **2024**, *34*, 2401228. [CrossRef]

77. James, A.M.; Gicevicius, M.; Hofer, S.; Schrode, B.; Werze, O.; Devaux, F.; Geerts, Y.H.; Sirringhaus, H.; Resel, R. Thin film crystallization of oligoethylene glycol-benzothieno benzothiophene: Physical vapor deposition versus spin coating. *J. Cryst. Growth* **2024**, *627*, 127539. [CrossRef]
78. Ko, F.Y.; Chiu, T.W.; Wu, R.T.; Chen, T.C.; Wang, S.H.; Chang, H.Y. Thin layer electrolyte impregnation into porous anode-supported fuel cell by ultrasonic spray pyrolysis. *Int. J. Hydrogen Energy* **2021**, *46*, 16708–16716. [CrossRef]
79. Carey, T.; Jones, C.; Moal, F.L.; Deganello, D.; Torrisi, F. Spray-Coating Thin Films on Three-Dimensional Surfaces for a Semitransparent Capacitive Touch Device. *ACS Appl. Mater. Interfaces* **2018**, *10*, 19948–19956. [CrossRef]
80. McGinn, P.J. Thin-film processing routes for combinatorial materials investigations—A review. *ACS Comb. Sci.* **2019**, *21*, 501–515. [CrossRef]
81. Mao, S.S.; Burrows, P.E. Combinatorial screening of thin film materials: An overview. *J. Mater.* **2015**, *1*, 85–91. [CrossRef]
82. Chiu, T.W.; Wakiya, N.; Shinozaki, K.; Mizutani, N. Effects of ambient gas and film thickness on orientation and surface morphology of $Sr_{0.5}Ba_{0.5}Nb_2O_6$ thin films prepared by pulsed laser deposition. *J. Ceram. Soc. Jpn.* **2002**, *110*, 368–372. [CrossRef]
83. Chiu, T.W.; Tonooka, K.; Kikuchi, N. Fabrication of transparent $CuCrO_2$:Mg/ZnO p–n junctions prepared by pulsed laser deposition on glass substrate. *Vacuum* **2009**, *83*, 614–617. [CrossRef]
84. Chiu, T.W.; Tonooka, K.; Kikuchi, N. Fabrication of ZnO and $CuCrO_2$:Mg thin films by pulsed laser deposition with in situ laser annealing and its application to oxide diodes. *Thin Solid Films* **2008**, *516*, 5941–5947. [CrossRef]
85. Chiu, T.W.; Tonooka, K.; Kikuchi, N. Influence of oxygen pressure on the structural, electrical and optical properties of VO_2 thin films deposited on ZnO/glass substrates by pulsed laser deposition. *Thin Solid Films* **2010**, *518*, 7441–7444. [CrossRef]
86. Tonooka, K.; Chiu, T.W.; Kikuchi, N. Preparation of transparent conductive TiO_2:Nb thin films by pulsed laser deposition. *Appl. Surf. Sci.* **2009**, *255*, 9695–9698. [CrossRef]
87. Varadarajan, V.; Norton, D. $CuGaO_2$ thin film synthesis using hydrogen-assisted pulsed laser deposition. *Appl. Phys. A* **2006**, *85*, 117–120. [CrossRef]
88. Nagata, T.; Chikyow, T. Combinatorial Synthesis Applied to the Development of Thin Film Materials for Nanoelectronics. In *Functional Thin Films Technology*, 1st ed.; CRC Press: Boca Raton, FL, USA, 2021; ISBN 9781003088080.
89. He, W.; Zhao, Y.; Xiong, Y. Bilayer Polyaniline-WO_3 Thin Film Sensors Sensitive to NO_2. *ACS Omega* **2020**, *5*, 9744–9751. [CrossRef]
90. Bruno, L.; Pijolat, C.; Lalauze, R. Tin dioxide thin-film gas sensor prepared by chemical vapour deposition Influence of grain size and thickness on the electrical properties. *Sens. Actuators B Chem.* **1994**, *18*, 195–199. [CrossRef]
91. Chen, C.Y.; Sakthinathan, S.; Yu, C.L.; Wang, C.C.; Chiu, T.W.; Han, Q. Preparation and characterization of delafossite $CuCrO_2$ film on flexible substrate. *Ceram. Int.* **2021**, *47*, 23234–23239. [CrossRef]
92. Chiu, T.-W.; Wakiya, N.; Shinozaki, K.; Mizutani, N. Effects of heating process on crystalline orientation and electrical properties of $(Bi, La)_4Ti_3O_{12}$ thin films derived by chemical solution deposition method. *Integr. Ferroelectr.* **2004**, *62*, 189–192. [CrossRef]
93. Chiu, T.W.; Chen, Y.A.; Lee, H.C.; Hong, S.Z. Preparing and applying nanosheets in controlling the orientation of TiO_2 thin films. *Ceram. Int.* **2015**, *41*, S213–S217. [CrossRef]
94. Bao, D.; Chiu, T.W.; Wakiya, N.; Shinozaki, K.; Mizutani, N. Structural and electrical characteristics of chemical-solution-derived $(Bi, La)_4Ti_3O_{12}$ thin films with various Bi_2O_3 template layers. *J. Appl. Phys.* **2003**, *93*, 497–503. [CrossRef]
95. Tampo, H.; Shibata, H.; Maejima, K.; Chiu, T.-W.; Itoh, H.; Yamada, A.; Matsubara, K.; Fons, P.; Chiba, Y.; Wakamatsu, T.; et al. Band profiles of ZnMgO/ZnO heterostructures confirmed by Kelvin probe force microscopy. *Appl. Phys. Lett.* **2009**, *94*, 242107. [CrossRef]
96. Weigenrieder, K. Conductivity model for sputtered ZnO-thin film gas sensors. *Thin Solid Films* **1997**, *300*, 30–41. [CrossRef]
97. Tao, W.; Tsai, C. H_2S sensing properties of noble metal doped WO_3 thin film sensor fabricated by micromachining. *Sens. Actuators B Chem.* **2002**, *81*, 237–247. [CrossRef]
98. Chiu, Y.; Tseng, C.; Lee, C. Nanostructured EGFET pH Sensors With Surface-Passivated ZnO Thin-Film and Nanorod Array. *IEEE Sens. J.* **2012**, *12*, 930–934. [CrossRef]
99. Liu, N.; Liu, Y.; Zhu, L.; Shi, Y.; Wan, Q. Low-Cost pH Sensors Based on Low-Voltage. *IEEE Electron Device Lett.* **2014**, *35*, 482–484. [CrossRef]
100. Chou, J.; Yan, S.; Liao, Y.; Lai, C. Characterization of flexible arrayed pH sensor based on nickel Oxide films. *IEEE Sens. J.* **2018**, *18*, 605–612. [CrossRef]
101. Kumar, N.; Kumar, J.; Panda, S. Enhanced pH sensitivity over the Nernst limit of electrolyte gated a-IGZO thin film transistor using branched polyethylenimine. *RSC Adv.* **2016**, *6*, 10810–10815. [CrossRef]
102. Bae, J. An elaborate sensor system based on conducting polymer-oligosaccharides in hydrogel and the formation of inclusion complexes. *J. Ind. Eng. Chem.* **2020**, *90*, 266–273. [CrossRef]
103. Jiang, C.; Li, Y.; Wang, H.; Chen, D.; Wen, Y. A portable visual capillary sensor based on functional DNA crosslinked hydrogel for point-of-care detection of lead ion. *Sens Actuators B Chem.* **2020**, *307*, 127625. [CrossRef]
104. Wang, H.; Wang, H.; Li, Y.; Jiang, C.; Chen, D.; Wen, Y.; Li, Z. Chemical capillarity self-driven DNA hydrogel sensor for visual quantification of microRNA. *Sens Actuators B Chem.* **2020**, *313*, 128036. [CrossRef]

105. Salikhov, R.; Lachinov, A. Polymer thin film chemical sensors. *Adv. Chem. Eng.* **2010**, *10*, 215–234.
106. Liu, R.; Wang, H.; Lu, W.; Cui, L.; Wang, S.; Wang, Y.; Chen, Q.; Guan, Y.; Zhang, Y. Highly tough stretchable and resilient hydrogels strengthened with molecular springs and their application as a wearable flexible sensor. *J. Chem. Eng.* **2021**, *415*, 128839. [CrossRef]
107. Yang, X.; Johnson, S.; Shi, J.; Holesinger, T.; Swanson, B. Polyelectrolyte and molecular host ion self-assembly to multilayer thin films: An approach to thin film chemical sensors. *Sens Actuators B Chem.* **1997**, *45*, 87–92. [CrossRef]
108. Keefe, M.H.; Slone, R.V.; Hupp, J.T.; Czaplewski, K.F.; Snurr, R.Q.; Stern, C.L. Mesoporous thin films of 'Molecular Squares' as sensors for volatile organic compounds. *Langmuir* **2000**, *16*, 3964–3970. [CrossRef]
109. Dandeneau, C.S.; Jeon, Y.; Shelton, C.T.; Plant, T.K.; Cann, D.P.; Gibbons, B. Thin film chemical sensors based on p-CuO/n-ZnO heterocontacts. *Thin Solid Films* **2009**, *517*, 4448–4454. [CrossRef]
110. Deshwal, M.; Arora, A. Enhanced acetone detection using Au doped ZnO thin film sensor. *J. Mater. Sci. Mater. Electron.* **2018**, *29*, 15315–15320. [CrossRef]
111. Eom, T.H.; Han, J.I. The effect of the nickel and chromium concentration ratio on the temperature coefficient of the resistance of a Ni–Cr thin film-based temperature sensor. *Sens. Actuators A Phys.* **2017**, *260*, 198–205. [CrossRef]
112. Ebner, M.; Ziegltrum, A.; Lohner, T.; Michaelis, K.; Stahl, K. Measurement of EHL temperature by thin film sensors Thermal insulation effects. *Tribol. Int.* **2020**, *149*, 105515. [CrossRef]
113. Hou, K.; Nie, Y.; Mugaanire, I.T.; Guo, Y.; Zhu, M. A novel leaf inspired hydrogel film based on fiber reinforcement as rapid steam sensor. *Chem. Eng. J.* **2020**, *382*, 122948. [CrossRef]
114. An, R.; Zhang, X.; Han, L.; Wang, X.; Zhang, Y.; Shi, L.; Ran, R. Healing, flexible, high thermal sensitive dual-network ionic conductive hydrogels for 3D linear temperature sensor. *Mater. Sci. Eng. C* **2020**, *107*, 110310. [CrossRef]
115. Lowe, M.; Hood, E.; Ozog, M. Thin-film force sensors: Opening doors in automated systems. *Sens. Rev.* **2007**, *27*, 99–102. [CrossRef]
116. Nadvi, G.S.; Butler, D.P.; Butler, Z.Ç.; Gönenli, I.E. Micromachined force sensors using thin film nickel chromium piezo resistors. *J. Micromechanics Microengineering* **2012**, *22*, 065002. [CrossRef]
117. Dumstorff, G.; Sarma, M.; Reimers, M.; Kolkwitz, B.; Brinksmeier, E.; Heinzel, C.; Lang, W. Steel integrated thin film sensors for characterizing grinding processes. *Sens. Actuators A Phys.* **2016**, *242*, 203–209. [CrossRef]
118. Asadnia, M. High temperature characterization of PZT(0.52'750.48) thin-film pressure sensors. *J. Micromechanics Microengineering* **2014**, *24*, 015017. [CrossRef]
119. Jing, X.; Li, H.; Mi, H.; Liu, Y.; Feng, P.; Tan, Y. Highly transparent, stretchable, and rapid self-healing polyvinyl alcohol/cellulose nano fibril hydrogel sensors for sensitive pressure sensing and human motion detection. *Sens. Actuators B Chem.* **2019**, *295*, 159–167. [CrossRef]
120. Shin, K.; Lee, J.S.; Jang, J. Highly sensitive, wearable and wireless pressure sensor using free-standing ZnO nanoneedle/PVDF hybrid thin film for heart rate monitoring. *Nano Energy* **2016**, *22*, 95–104. [CrossRef]
121. Li, Q.; Luo, S.; Wang, Q. Piezoresistive thin film pressure sensor based on carbon nanotube-polyimide nanocomposites. *Sens. Actuators A Phys.* **2019**, *295*, 336–342. [CrossRef]
122. Yuk, J.; Troczynski, T. Sol–gel $BaTiO_3$ thin film for humidity sensors. *Sens Actuators B Chem.* **2003**, *94*, 290–293. [CrossRef]
123. Islam, T.; Khan, F.A.; Khan, S.A.; Saha, H. A Sensitive Digital Moisture Detector For Nanostructured Thin Film Sensor. *Int. J. Smart Sens. Intell. Syst.* **2014**, *7*, 1059–1076. [CrossRef]
124. Mittal, U.; Islam, T.; Nimal, A.T.; Sharma, M.U. A Novel Sol-Gel γ -Al_2O_3 Thin-Film-Based. *IEEE Trans. Electron Dev.* **2015**, *62*, 4242–4250. [CrossRef]
125. Mahboob, R.; Zargar, Z.H.; Islam, T. A sensitive and highly linear capacitive thin film sensor for trace moisture measurement in gases. *Sens. Actuators B Chem.* **2016**, *228*, 658–664. [CrossRef]
126. Jiang, M.; Gerhard, E. A simple strain sensor using a thin film as a low-finesse fiber-optic fabry perot interferometer. *Sens. Actuators A-Phys.* **2001**, *88*, 41–46. [CrossRef]
127. Stephen, R.J.; Rajanna, K.; Dhar, V.; Kumar, K.G.K.; Nagabushanam, S. Thin-film strain gauge sensors for ion thrust measurement. *IEEE Sens. J.* **2004**, *4*, 373–377. [CrossRef]
128. Frommberger, M.; Glasmachers, S.; Schmutz, C.; Mccord, J. Microscopic magnetic and high-frequency properties of a stress sensor using FeCoBSi magneto strictive thin films. *IEEE Trans. Magn.* **2005**, *41*, 3691–3693. [CrossRef]
129. Wang, Y.; Tebyetekerwa, M.; Liu, Y.; Wang, M.; Zhu, J.; Xu, J.; Zhang, C.; Liu, T. Extremely stretchable and healable ionic conductive hydrogels fabricated by surface competitive coordination for human-motion detection. *J. Chem. Eng.* **2021**, *420*, 127637. [CrossRef]
130. Han, L.; Liu, M.; Yan, B.; Li, Y.; Lan, J.; Shi, L.; Ran, R. Polydopamine/polystyrene nanocomposite double-layer strain sensor hydrogel with mechanical, self-healing, adhesive and conductive properties. *Mater. Sci. Eng. C* **2020**, *109*, 110567. [CrossRef] [PubMed]

131. Zhou, H.; Jin, Z.; Yuan, Y.; Zhang, G.; Zhao, W.; Jin, X. Self-repairing flexible strain sensors based on nanocomposite hydrogels for whole-body monitoring. *Colloids Surf. A* **2020**, *592*, 124587. [CrossRef]
132. Togawa, K.; Sanbonsugi, H.; Lapicki, A.; Abe, M.; Handa, H. High-sensitivity InSb thin-film micro-hall sensor arrays for simultaneous multiple detection of magnetic beads for biomedical applications. *IEEE Trans. Magn.* **2005**, *41*, 3661–3663. [CrossRef]
133. Kim, J.; Lee, J.; Lee, H.; Oh, I. Nano energy stretchable and self-healable catechol-chitosan-diatom hydrogel for triboelectric generator and self-powered tremor sensor targeting at Parkinson disease. *Nano Energy* **2021**, *82*, 105705. [CrossRef]
134. Li, S.Y.; Kim, Y.G.; Jung, S.; Song, S.H.; Lee, S.M. Application of steel thin film electrical resistance sensor for in situ corrosion monitoring. *Sens Actuators B Chem.* **2007**, *120*, 368–377. [CrossRef]
135. Wright, R.F.; English, R.; Egbu, J.C.; Baltrus, J.; Moroz, M.Z.; Ohodnicki, P.R. Fe thin film-coated optics for corrosion monitoring: Optical and electrochemical studies. *JOM* **2021**, *73*, 655–664. [CrossRef]
136. Sanmugam, A.; Vikraman, D.; Karuppasamy, K.; Lee, J.Y.; Kim, H.S. Evaluation of the corrosion resistance properties of electroplated chitosan $Zn_{1-x}Cu_xO$ composite thin films. *Nanomaterials* **2017**, *7*, 432. [CrossRef]
137. Zhu, Z.; Liu, X.; Ye, Z.; Zhang, J.; Cao, F.; Zhang, J. A fabrication of iridium oxide film pH micro-sensor on Pt ultramicroelectrode and its application on in-situ pH distribution of 316L stainless steel corrosion at open circuit potential. *Sens. Actuators B Chem.* **2018**, *255*, 1974–1982. [CrossRef]
138. Yao, Z.J. Single crystal silicon supported thin film micromirrors for optical applications. *Opt. Eng.* **1997**, *36*, 1408–1413. [CrossRef]
139. Sakata, M.; Wakabayashi, S.; Ikeda, M.; Goto, H.; Takeuchi, M.; Yada, T. Pb-based ferroelectric thin film actuator for optical applications. *Microsyst. Technol.* **1995**, *2*, 26–31. [CrossRef]
140. Shkir, M. Linear, Third order nonlinear and optical limiting studies on MZO/FTO thin film system fabricated by spin coating technique for electro-optic applications. *J. Mater. Res.* **2018**, *33*, 3880–3889. [CrossRef]
141. Villar, I.D.; Arregui, F.J.; Ozcariz, A.; Dominik, M.; Smietana, M.; Zamarre, C.R. Lossy mode resonance optical sensors based on indium-gallium-zinc oxide thin film. *Sens. Actuators A-Phys.* **2019**, *290*, 20–27.
142. Khalil, M.M.; Sayed, A.H.E.; Masoud, M.S.; Mahmoud, E.M.; Hamad, M.A. Synthesis and optical properties of alizarin yellow GG Cu (II) -PVA nanocomposite film as elective filter for optical applications. *J. Mater. Res. Technol.* **2021**, *11*, 33–39. [CrossRef]
143. Manera, M.G.; Spadavecchia, J.; Buso, D.; de Julián Fernández, C.; Mattei, G.; Martucci, A.; Mulvaney, P.; Pérez-Juste, J.; Rella, R.; Vasanelli, L.; et al. Optical gas sensing of TiO_2 and TiO_2/Au nanocomposite thin films. *Sens. Actuators B-Chem.* **2008**, *132*, 107–115. [CrossRef]
144. Nechibvute, A.; Chawanda, A.; Luhanga, P. Piezoelectric energy harvesting devices: An alternative energy source for wireless Sensors. *Smart Mater. Res.* **2012**, *2012*, 853481. [CrossRef]
145. Khan, A.; Abas, Z.; Kim, H.S.; Oh, I.K. Piezoelectric thin films: An integrated review of transducers and energy harvesting. *Smart Mater. Struct.* **2016**, *25*, 053002. [CrossRef]
146. Han, Z.; Song, C.; Zhou, J.; Ma, Z.; Ma, L.; Gao, H.; Zheng, F. Influence of the deposition conditions on the magnetic properties of Fe–Co–N thin films. *J. Alloys Compd.* **2023**, *934*, 167951. [CrossRef]
147. Bi, Z.; Zhang, Z.; Fan, P. Effect of sputter deposition parameters on the characteristics of PZT ferroelectric thin films. *J. Phys. Conf. Ser.* **2007**, *61*, 115–119. [CrossRef]
148. Zhang, Y.; Dong, C.; Yang, S.; Chiu, T.W.; Wu, J.; Xiao, K.; Huang, Y.; Li, X. Enhanced silver loaded antibacterial titanium implant coating with novel hierarchical effect. *J. Biomater. Appl.* **2018**, *32*, 1289–1299. [CrossRef] [PubMed]
149. Wang, Y.P.; Chiu, T.W.; Chang, C.H.; Xuan, C.; Cheng, G.J. Transparent and antibacterial $Cu_2Y_2O_5$ thin films by chemical solution deposition. *Thin Solid Films* **2014**, *570*, 547–551. [CrossRef]
150. Barote, M.A.; Yadav, A.A.; Masumdar, E.U. Effect of deposition parameters on growth and characterization of chemically deposited cd1-xpbxs thin films. *Chalcogenide* **2011**, *8*, 129.
151. Gojzewski, H.; Ghani, F.; Szybowicz, M. Thin films of copper phthalocyanine deposited by solution processing methods. *Mater. Sci.* **2020**, *38*, 79–90. [CrossRef]
152. Ghani, F.; Gojzewski, H.; Riegler, H. Nucleation and growth of copper phthalocyanine aggregates deposited from solution on planar surfaces. *Appl. Surf. Sci.* **2015**, *351*, 969–976. [CrossRef]
153. Ghani, F.; Bochukov, I.; Fostiropoulos, K.; Riegler, H. Hybrid solution/vacuum-processed bilayer heterojunction organic solar cells: Structural characterization and performance. *Thin Solid Films* **2012**, *525*, 177–181. [CrossRef]
154. Ingrosso, C.; Curri, M.L.; Fini, P.; Giancane, G.; Agostiano, A.; Valli, L. Functionalized Copper (II)−Phthalocyanine in Solution and As Thin Film: Photochemical and Morphological Characterization toward Applications. *Langmuir* **2009**, *25*, 10305–10313. [CrossRef] [PubMed]
155. Lee, J.H.; Kim, S.; Kim, H.; Lee, J. Solvent-dependent performance of solution-processed small-molecule organic field-effect transistors. *Org. Electron.* **2018**, *52*, 184–189. [CrossRef]
156. Kim, Y.H.; Lee, Y.U.; Han, J.I.; Han, S.M.; Han, M.K. Influence of solvent on the film morphology, crystallinity and electrical characteristics of triisopropylsilyl pentacene OTFTs. *J. Electrochem. Soc.* **2007**, *154*, H995. [CrossRef]

157. Rubinger, C.P.L.; Haneef, H.F.; Hewitt, C.; Carroll, D.; Anthony, J.E.; Jurchescu, O.D. Influence of solvent additives on the morphology and electrical properties of diF-TES ADT organic field-effect transistors. *Org. Electron.* **2019**, *68*, 205–211. [CrossRef]
158. Christensen, T.M. *Understanding Surface and Thin Film Science*; CRC Press: Boca Raton, FL, USA, 2022. [CrossRef]
159. Kaiser, N. Review of the fundamentals of thin-film growth. *Appl. Opt.* **2002**, *41*, 16. [CrossRef]
160. Bard, A.J.; Stratmann, M.; Rubinstein, I.; Fujihira, M.; Rusling, J.F. (Eds.) Modified Electrodes. In *Encyclopedia of Electrochemistry*; Wiley-VCH: Weinheim, Germany, 2007; Volume 10.
161. Xu, X.; Tian, B.; Zhang, S.; Kong, J.; Zhao, D.; Liu, B. Electrochemistry and biosensing reactivity of heme proteins adsorbed on the structure-tailored mesoporous Nb_2O_5 matrix. *Anal. Chim. Acta* **2004**, *519*, 31–38. [CrossRef]
162. Topoglidis, E.; Campbell, C.J.; Cass, A.E.G.; Durrant, J.R. Nitric oxide Biosensors Based on the Immobilization of Hemoglobin on Mesoporous Titania Electrodes. *Electroanalysis* **2006**, *18*, 882–887. [CrossRef]
163. Feng, J.J.; Xu, J.J.; Chen, H.Y. Direct electron transfer and electrocatalysis of hemoglobin adsorbed onto electrodeposited mesoporous tungsten oxide. *Electrochem. Commun.* **2006**, *8*, 77. [CrossRef]
164. Yu, J.; Ma, J.; Zhao, F.; Zeng, B. Direct electron-transfer and electrochemical catalysis of hemoglobin immobilized on mesoporous Al_2O_3. *Electrochim. Acta* **2007**, *53*, 1995. [CrossRef]
165. Lunsford, S.K.; Choi, H.; Stinson, J.; Yeary, A.; Dionysiou, D.D. Voltammetric determination of catechol using a sonogel carbon electrode modified with nanostructured titanium dioxide. *Talanta* **2007**, *73*, 172–177. [CrossRef] [PubMed]
166. Kumar, P.; Kim, K.H.; Vellingiri, K.; Samaddar, P.; Kumar, P.; Deep, A.; Kumar, N. Hybrid porous thin films: Opportunities and challenges for sensing applications. *Biosens. Bioelectron.* **2018**, *104*, 120–137. [CrossRef]
167. Wang, Y.; Wu, X.; Li, Y.; Zhou, Z. Mesostructured SnO_2 as sensing material for gas sensors. *Solid State Electron.* **2004**, *48*, 627–632. [CrossRef]
168. Xu, Q.; Zhu, J.J.; Hu, X.Y. Ordered mesoporous polyaniline film as a new matrix for enzyme immobilization and biosensor construction. *Anal. Chim. Acta* **2007**, *597*, 151–156. [CrossRef] [PubMed]
169. Bilewicz, R.; Rowinski, P.; Rogalska, E. Modified electrodes based on lipidic cubic phases. *Bioelectrochemistry* **2005**, *66*, 3–8. [CrossRef] [PubMed]
170. Zhou, M.; Ding, J.; Guo, L.; Shang, Q. Electrochemical behavior of L-Cysteine and its detection at ordered mesoporous carbon-modified glassy carbon electrode. *Anal. Chem.* **2007**, *79*, 5328–5335. [CrossRef]
171. Bertolo, J.M.; Bearzotti, A.; Falcaro, P.; Traversa, E.; Innocenzi, P. Sensoristic applications of self-assembled mesostructured silica films. *Sens. Lett.* **2003**, *1*, 64–70. [CrossRef]
172. Bertolo, J.M.; Bearzotti, A.; Generosi, A.; Palummo, L.; Albertini, V.R. X-rays and electrical characterizations of ordered mesostructurated silica thin films used as sensing membranes. *Sens. Actuators B* **2005**, *111–112*, 145–149. [CrossRef]
173. Zhang, L.; Zhang, Q.; Li, J. Direct electrochemistry and electrocatalysis of hemoglobin immobilized in bimodal mesoporous silica and chitosan inorganic–organic hybrid film. *Electrochem. Commun.* **2007**, *9*, 1530–1535. [CrossRef]
174. Zhang, X.; Wang, J.; Wu, W.; Qian, S.; Man, Y. Immobilization and electrochemistry of cytochrome c on amino-functionalized mesoporous silica thin films. *Electrochem. Commun.* **2007**, *9*, 2098–2104. [CrossRef]
175. Dai, Z.H.; Ni, J.; Huang, X.H.; Lu, G.F.; Boa, J.C. Direct electrochemistry of glucose oxidase immobilized on a hexagonal mesoporous silica-MCM-41 matrix. *Bioelectrochemistry* **2007**, *70*, 250. [CrossRef]
176. Dai, Z.; Liu, S.; Ju, H.; Chen, H. Direct electron transfer and enzymatic activity of hemoglobin in a hexagonal mesoporous silica matrix. *Biosens. Bioelectron.* **2004**, *19*, 861. [CrossRef]
177. Domenech, A.; Garcia, H.; Marquet, J.; Bourdelande, J.L.; Herance, J.R. Modelling electrocatalysis of hydroquinone oxidation by nicotinamide adenine dinucleaotide coenzyme encapsulated within SBA-15 and MCM-41 mesoporous aluminosilicates. *Electrochim. Acta* **2006**, *51*, 4897–4908. [CrossRef]
178. Yu, J.J.; Lu, S.; Li, J.W.; Zhao, F.Q.; Zeng, B.Z. Characterization of gold nanoparticles electrochemically deposited on amine-functioned mesoporous silica films and electrocatalytic oxidation of glucose. *J. Solid State Electrochem.* **2007**, *11*, 1211–1219. [CrossRef]
179. Yantasee, W.; Lin, Y.; Li, X.; Fryxell, G.E.; Zemanian, T.S.; Viswanathan, V.V. Nanoengineered electrochemical sensor based on mesoporous silica thin-film functionalized with thiol-terminated monolayer. *Analyst* **2003**, *128*, 899. [CrossRef]
180. Etienne, M.; Walcarius, A. Evaporation induced self-assembly of templated silica and organosilica thin films on various electrode surfaces. *Electrochem. Commun.* **2005**, *7*, 1449–1456. [CrossRef]
181. Etienne, M.; Cortot, J.; Walcarius, A. Preconcentration electroanalysis at surfactant-templated thiol-functionalized silica thin films. *Electroanalysis* **2007**, *19*, 129–138. [CrossRef]
182. Tchinda, A.J.; Ngameni, E.; Walcarius, A. Thiol-functionalized porous clay heterostructures (PCHs) deposited as thin films on carbon electrode: Towards mercury(II) sensing. *Sens. Actuators B* **2007**, *121*, 113–123. [CrossRef]
183. Voicu, A.I.; Garea, S.A.; Ghebaur, A.; Nistor, C.L.; Sarbu, A.; Vasile, E.; Mitran, R.; Iovu, H. New nanocarriers based on porous clay heterostructures (PCH) designed for methotrexate delivery. *Microporous Mesoporous Mater.* **2021**, *328*, 111434. [CrossRef]

184. Sberveglieri, G. Recent developments in semiconducting thin-film gas sensors. *Sens. Actuators B-Chem.* **1995**, *23*, 103–109. [CrossRef]
185. Li, S.; Ahuja, R.; Barsoum, M.W.; Jena, P.; Johansson, B. Optical properties of Ti_3SiC_2 and Ti_4AlN_3. *Appl. Phys. Lett.* **2008**, *92*, 221907. [CrossRef]
186. Rondinelli, J.M.; Spaldin, N.A. Structure and properties of functional oxide thin films: Insights from electronic-structure calculations. *Adv. Mater.* **2011**, *23*, 3363–3381. [CrossRef]
187. Sulka, G.D. Electrochemistry of thin films and nanostructured materials. *Molecules* **2023**, *28*, 4040. [CrossRef]
188. Mroczka, R.; Słodkowska, A.; Ladniak, A. Studies of bis-(sodium-sulfopropyl)-disulfide and 3-mercapto-1-propanesulfonate on/into the copper electrodeposited layer by time-of-flight secondary-ion mass spectrometry. *Molecules* **2022**, *27*, 8116. [CrossRef] [PubMed]
189. Mroczka, R.; Słodkowska, A.; Ladniak, A.; Chrzanowska, A. Interaction of bis-(sodium-sulfopropyl)-disulfide and polyethylene glycol on the copper electrodeposited layer by time-of-flight secondary-ion mass spectrometry. *Molecules* **2023**, *28*, 433. [CrossRef]
190. Saito, N.; Yamamoto, T. Poly(l,5-naphthyridine-2,6-diyl) having a highly extended and electron-withdrawing p-conjugation system. Preparation, optical properties, and electrochemical redox reaction. *Macromolecules* **1995**, *28*, 4260–4267. [CrossRef]
191. Keller, F.; Hunter, M.S.; Robinson, D.L. Structural features of oxide coatings on aluminum. *J. Electrochem. Soc.* **1953**, *100*, 411–419. [CrossRef]
192. Masuda, H.; Satoh, M. Fabrication of gold nanodot array using anodic porous alumina as an evaporation mask. *JPN J. Appl. Phys.* **1996**, *35*, L126–L129. [CrossRef]
193. Sulka, G.D. Introduction to anodization of metals. In *Nanostructured Anodic Metal Oxides, Synthesis and Applications*; Sulka, G.D., Ed.; Elsevier: Amsterdam, The Netherlands, 2020; pp. 1–34.
194. Ono, S. Nanostructure analysis of anodic films formed on aluminum-focusing on the effects of electric field strength and electrolyte anions. *Molecules* **2021**, *26*, 7270. [CrossRef]
195. Biswas, A.; Natu, V.; Puthirath, A.B. Thin-film growth of MAX phases as functional materials. *Oxf. Open Mater. Sci.* **2021**, *1*, itab020. [CrossRef]
196. Barsoum, M.W. The $M_{N+1}AX_N$ phases: A new class of solids. *Prog. Solid State Chem.* **2000**, *28*, 201–280. [CrossRef]
197. Radovic, M.; Barsoum, M.W. MAX phases: Bridging the gap between metals and ceramics. *Am. Ceram. Soc. Bull.* **2013**, *92*, 20.
198. Fu, L.; Xia, W. MAX phases as nanolaminate materials: Chemical composition, microstructure, synthesis, properties, and applications. *Adv. Eng. Mater.* **2021**, *23*, 2001191. [CrossRef]
199. Sokol, M.; Natu, V.; Kota, S.; Barsoum, M.W. On the chemical diversity of the MAX phases. *Trends Chem.* **2019**, *1*, 210–223. [CrossRef]
200. Mauchamp, V.; Yu, W.; Gence, L.; Piraux, L.; Cabioc, T.; Gauthier, V.; Eklund, P.; Dubois, S. Anisotropy of the resistivity and charge-carrier sign in nano laminated Ti_2AlC: Experiment and ab initio calculations. *Phys. Rev. B* **2013**, *87*, 235105. [CrossRef]
201. Pinek, D.; Ito, T.; Furuta, K.; Kim, Y.; Ikemoto, M.; Ideta, S.-I.; Tanaka, K.; Nakatake, M.; Le Fèvre, P.; Bertran, F.; et al. Near Fermi level electronic structure of Ti_3SiC_2 revealed by angle-resolved photoemission spectroscopy. *Phys. Rev. B* **2020**, *102*, 075111. [CrossRef]

Disclaimer/Publisher's Note: The statements, opinions and data contained in all publications are solely those of the individual author(s) and contributor(s) and not of MDPI and/or the editor(s). MDPI and/or the editor(s) disclaim responsibility for any injury to people or property resulting from any ideas, methods, instructions or products referred to in the content.